UNIVERSITY OF TWENTE.

Faculty of Electrical Engineering,
Mathematics & Computer Science

Comparison of medium access control protocols for ultra narrowband communication systems

Leon Schenk

M.Sc. Thesis
August 2017

Supervisors:
prof. dr. ir. ing. Frank Leferink
dr. ir. Mark Bentum
dr. ir. Arjan Meijerink
Zaher Mahfouz M.Sc.
dr. ir. Pieter-Tjerk de Boer

Telecommunication Engineering Group
Faculty of Electrical Engineering,
Mathematics and Computer Science
University of Twente
P.O. Box 217
7500 AE Enschede
The Netherlands

Contents

List of acronyms

AWGN	additive white Gaussian noise
BER	bit error rate
BPSK	binary phase shift keying
CAES	Computer Architecture for Embedded Systems
CCA	clear channel assessment
CDMA	code division multiple access
CR-FDMA	continuous random frequency division multiple access
CRC	cyclic redundancy check
CSMA	carrier sense multiple access
FEC	forward error correction
FHSS	frequency hopping spread spectrum
FS-TS-Aloha	frequency slotted time slotted Aloha
FS-TU-Aloha	frequency slotted time unslotted Aloha
FOM	figure of merit
FU-TS-Aloha	frequency unslotted time slotted Aloha
FU-TU-Aloha	frequency unslotted time unslotted Aloha
ICD	Integrated Circuit Design
ID	Identifier
IF	intermediate frequency
ISI	inter symbol interference

ISMA	idle sense multiple access
LBT	listen before talk
LO	local oscillator
MAC	medium access control
OFDM	orthogonal frequency division multiplexing
OOK	on-off keying
OSI	open systems interconnection
PDR	packet delivery ratio
PER	packet error rate
PHY	physical layer
PLL	phase locked loop
PSD	power spectral density
QoS	quality of service
RF	radio frequency
RRC	root raised cosine
RSSI	received signal strength indication
RTS	request to send
SINR	signal to interference plus noise ratio
SIR	signal to interference ratio
TDMA	time division multiple access
TE	Telecommunication Engineering
UNB	ultra narrowband
WSN	wireless sensor network

Chapter 1

Introduction

In this chapter the background information (Section 1.1 for this work is presented. Then from the motivation (Section 1.2) and the context (Section 1.3) of this research project an objective (Section 1.5) is formulated with its bounds given in Section 1.4.

1.1 Background

Due to improvements in technology over the last decades it has become possible to create integrated systems that sense the environment and take action on the collected data. This technology trend is given lots of attention and is driven further and further. The sensors of such a network are easy to deploy, autonomous and low in maintenance. Such networks are often referred to as wireless sensor networks (WSNs). The WSNs are used to collect sensor data from the environment and are especially effective in harsh environments or when having numerous sensors. Oppermann et al. [1] presented an overview of many such applications and propose a method to categorize WSN applications on the basis of their network requirements. The applications mentioned in [1] make use of customized networks to collect the required data. This customization step means that for each application a new network is designed. This process is very inefficient. It shows there is a market for a single network that is able to support the majority of applications. For WSN applications the existing networks (cellular network, WiFi access points, ZigBee or others) often do not suffice. This can be due to energy demands, availability of the network, cost, or any other limitation. According to Oppermann et al., the majority of applications (32 out of 62) are in the category 'low-rate data collection', have tens of nodes and require a lifetime up to years. The development of a network that targets the achievements of these constraints has been a major field of research [2]. The common features for networks of the low-rate data collection applications are a high number of nodes, up to years of lifetime, transmission from node to server and low average data rate. Time synchronization, localization, firmware update or reconfiguration are required services for some of the applications. These services can be solved in the network or can be left up to the node or application to be solved. In the latter case there is no requirement for the network, but it does increase demands on the node that might include additional transceivers or higher energy consumption. Drago et al. mentioned in [3] the main challenge for WSNs is to produce small, cheap and power autonomous nodes. A network which allows for energy efficient nodes is key to the success of a WSN, because transmission of data is a major factor in energy consumption of nodes. Many WSNs are finding their way to the market these days. Basically two approaches for exploitation of WSNs exist. There are those that let the infrastructure be supplied by third parties. And the ad hoc type networks, where the infrastructure is provided along with the sensor nodes by the user. One example of the former is the Sigfox network. This network uses a grid of base stations with a very high range, connected by a very powerful backbone. These type of networks are called star topology networks. To achieve this Sigfox uses ultra narrowband (UNB) binary phase shift keying (BPSK) modulation [4] in combination with a low symbol rate. Sigfox is a major player in the area of UNB communication for WSNs. A general model used to describe WSN layers, is the model shown in Figure 1.1. This model is quite similar to the well known open systems interconnection (OSI) model, with the difference of being modified for WSNs. This model is introduced because the challenges and requirements in WSN proved to be different to those of other networks, such as the Internet. The Internet has its main focus on reliability and high data rate. On the contrary; power management, mobility management and task management are very important factors to take into account in a WSN. The applications have to be able to deal with the consequences, the amount of traffic they generate is limited to reduce energy consumption while maintaining a high reliability. Each layer from Figure 1.1 has an implementation in either hardware or software and each has its own research goals and challenges.

Data link layer The data link layer is the lowest software layer. The goal of the data link layer is efficient use of the bandwidth and available energy at the node, while ensuring appropriate quality of service (QoS) for the upper layers. The data link layer is responsible for efficiently sharing access to the medium, this is done with a medium access control (MAC) protocol. There can be large differences between MAC protocols in how they share the medium. The choice of MAC protocol affects network performance and efficient spectrum use. Sharing a medium between a large amount of unsynchronized, unconnected nodes is a difficult task, since nodes are unable to express their wish to use the medium without accessing the medium itself. The MAC protocol determines when and how a node is allowed to access the medium. To do

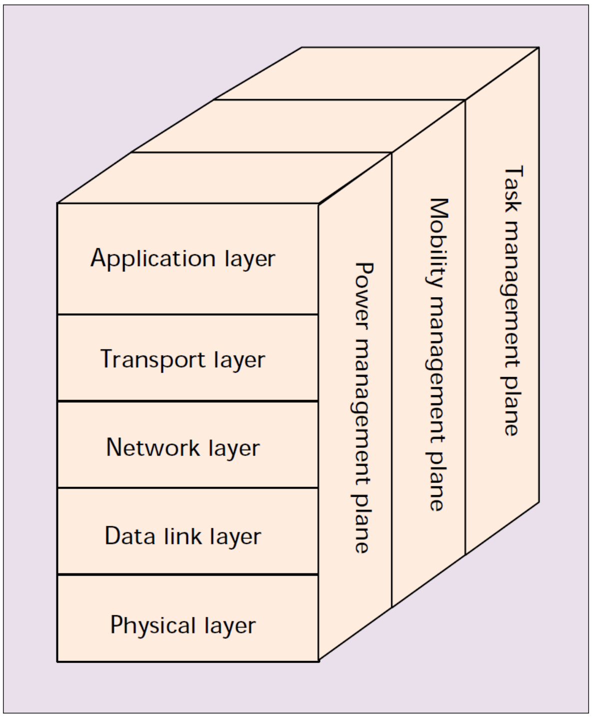

Figure 1.1: Layered model for a general WSN implementation [2].

this the medium is subdivided into multiple logical channels. The physical layer defines these logical channels to the data link layer, but unfortunately these channels are not free of errors. Noise, co-channel interference, adjacent channel interference and other effects can cause errors in received packets on the channel. For example, two nodes may decide to transmit using the same logical channel at the same time causing a collision at the receiver. Some MAC protocols make use of advanced features of the physical layer that they might not support. For example, when the physical layer (PHY) does not support received signal strength indication (RSSI) measurements, a listen before talk (LBT) type MAC protocol cannot be used. Other features may be code division multiple access (CDMA), frequency hopping spread spectrum (FHSS) or other multiplexing techniques.

Physical layer The physical layer of a wireless network consists of a hardware implementation of the radio frequency (RF) transceiver with a hardware interface with registers and connected interrupts. The modulation scheme, symbol rate, bit rate, pulse shaping, transmission frequency, and more are determined at this layer. A reference high level diagram of a physical layer is shown in Figure 1.2. The CC1021 is a configurable PHY layer chip for diverse networking tasks. It performs up and down conversion in analog domain, before processing the intermediate frequency (IF) digitally. Modulation, demodulation, pulse shaping, RSSI measurements and other are done digitally. Such a physical layer can be used to create prototype nodes for a

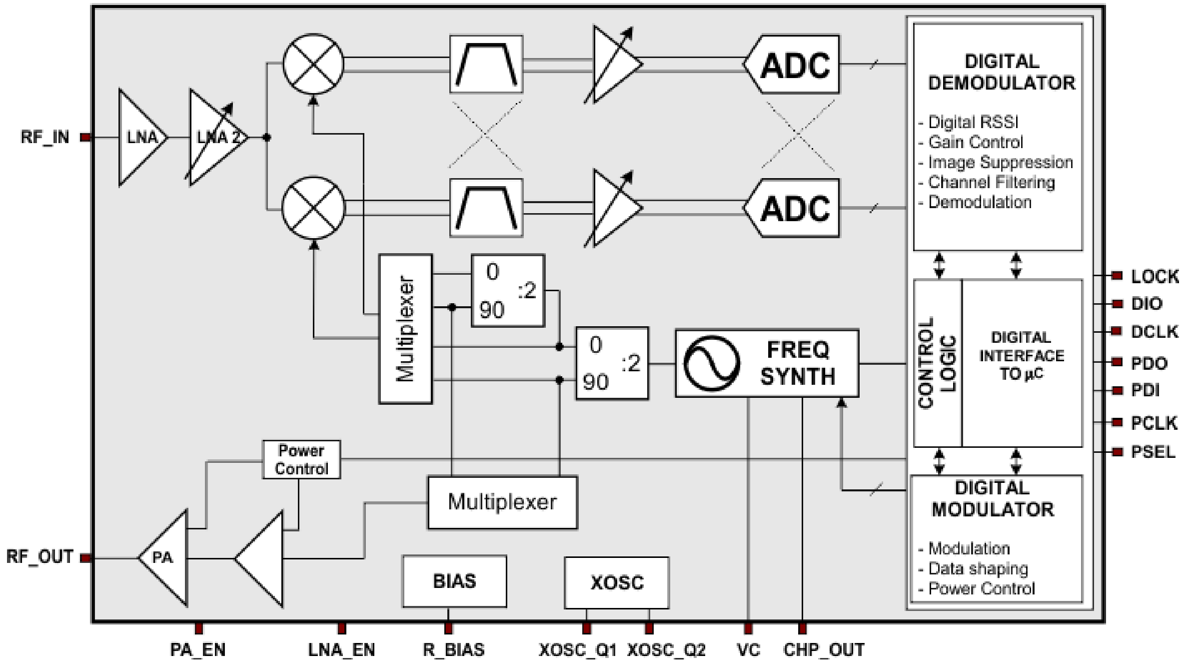

Figure 1.2: PHY reference implementation for WSN [5].

WSN. The choice of modulation parameters is important for optimization of the network performance. However, every decision has advantages and disadvantages. The choice of MAC protocol cannot be made independently from the choices in the physical layer.

1.2 Motivation

The area of WSNs has been given much attention in recent years. The WSNs seem to fill a gap for large scale networks with huge amounts of nodes and relatively low datarate per node. Existing network technologies are not supporting this or exploitation at the intended scale is too expensive. Do et al. [6] mentioned the benefits of UNB. High link budget and low energy consumption are two interesting benefits of UNB for a long range, star topology network, such as that of Sigfox. The benefits of UNB make it a good candidate for the physical layer. The benefits on the physical layer are obvious from the available literature. However, little is known about MAC performance for such a network. Some research has been done to find out what physical effects influence MAC performance in a UNB network. However, the conclusions drawn by [6] are not in line with known benefits of other MAC protocols, such as carrier sense multiple access (CSMA) or time division multiple access (TDMA). Because of the long packet transmission times of UNB the energy consumption penalty for collision is considerably high. For example, CSMA has been shown to improve throughput and reduce packet collision probability in regular networks. Moreover, as Kleinrock et al. [7] pointed out as a major drawback of CSMA is the relative propagation time to the packet duration. However, as packet duration is factors higher than propagation time in UNB this disadvantage has little influence on CSMA performance. In contrast to conventional physical layers, in UNB frequency uncertainty is of major concern. For example, frequency uncertainty of a 10-ppm crystal in the 868-MHz band is 8680 Hz. This value may not be large when compared to the bandwidth of a regular channel in the 868-MHz band and adjacent channel interference can easily be reduced by increasing the guard band between channels. However, the bandwidth of a UNB signal can be as small as 100 Hz. This means either adjacent channel interference is high or the bandwidth is inefficiently used. Furthermore, compensation or synchronization of the frequency will result in higher energy consumption or overhead and is thus not feasible for WSNs. To the best of our knowledge, only [6] investigated the issue of frequency uncertainty quantitatively. As a conclusion of their work, they stress the fact that the effect of frequency uncertainty cannot be overlooked, where it concerns MAC protocol performance in a UNB network. A quantitative study including the effects of frequency uncertainty is required to evaluate the presumption that other known MAC protocols may perform better than the one proposed by Do.

1.3 Context

UNB is characterized by a low data rate and good performance under high interference conditions. From the power spectral density (PSD) of an UNB signal compared to a wideband interferer, seen in Figure 1.3, it can be noted here that the UNB signal is much stronger than that of the interferer. A UNB receiver will receive only a small portion of power of the wideband interference. This indicates a two way advantage in terms of interference rejection and improved range. The Telecommunication Engineering (TE) research group is engaged in a cooperation project called ”Slow Wireless”, together with the Integrated Circuit Design (ICD) and Computer Architecture for Embedded Systems (CAES) groups, to investigate whether a UNB network will be a feasible approach for low-rate data collection applications. This investigation is done through the development of a prototype node, which aims to fulfill the requirements and be optimally adapted for the targeted applications. This means the nodes are designed to be as power efficient, physically small and cheap as possible.

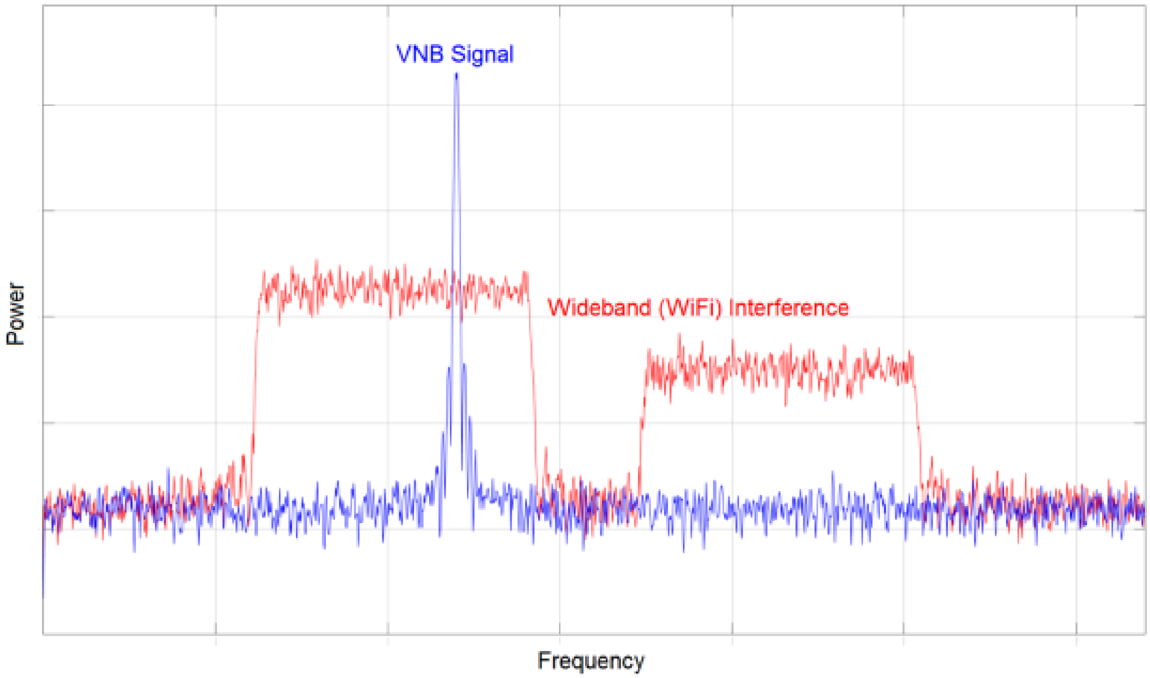

Figure 1.3: Capability of UNB to cope with interference [8].

1.4 Scope

This master thesis outlines an investigation on the performance of different types of MAC protocols in a UNB communication system. The method of access of a high number of unsynchronized wireless nodes to a single shared medium in an efficient manner can make a huge difference in overall network performance. Access to the medium from nodes to the base station in a star topology WSN is therefore a very important aspect of network design. In this work MAC protocols for uplink are compared with each other. The link from the base station to the nodes is not part of this. The downlink can be assumed perfect and not interfering with the uplink channel. Downlink is used for out-of-band signaling. Only the influence of the MAC layer is investigated. To do this the layers below this will be kept unchanged when comparing between different MAC protocols. The basic specifications of the physical layer of the Sigfox network are taken as a benchmark, because that network is a major player in UNB WSNs. This means the modulation type is BPSK, with a bit rate of 100 bps, root raised cosine pulse shaping and approximately 20 bytes data per packet. The downlink of the Sigfox network is not modeled and assumed perfect.

1.5 Objective

The objective for this thesis is to investigate which MAC protocol is most suitable for the uplink of a UNB communication system in a star topology network, given the relevant physical and hardware limitations for UNB, by making a comparison of available MAC protocols. To do this first a selection of suitable MAC protocols is performed. Selection criteria are presented based on the scope, such that only relevant MAC protocols are considered for comparison. The MAC protocols are compared on important, industry standard performance figures. The most relevant effects and limitations for UNB are included in the model to create a fair comparison of the available MAC protocols.

1.6 Report organization

The remainder of this report is organized as follows. In Chapter 2 the methodology is described, including assumptions made, the models used for fair comparison and the steps taken to reach the research objective. Then, in Chapter 3, the results of the method are presented. Comments and explanations are given in Chapter 4. And finally in Chapter 5 the conclusions of the work are drawn and recommendations are given for research projects that may follow up this work.

Chapter 2

Methodology

In this chapter, the method for the project is discussed. This answers the question of how the objective is achieved, keeping in mind the limitations and boundary conditions given in the scope. Furthermore the assumptions and models are presented in this chapter. The rough approach to fulfill the research objective is to first search for MAC protocols, and select those which are suitable for the scope of the project. Selection criteria are given in Section 2.1 and shows which MAC protocols are suitable for simulation and to what conditions the MAC protocol should adhere to. The model that describes the most important aspects of the UNB network is designed in Section 2.2. Because the model will be too complex for mathematical analysis the selected protocols of Section 2.1 will be subject of simulation. Which figure of merits (FOMs) are used to measure performance of the MAC protocol, is described in Section 2.3. If all FOMs are generated for all MAC protocols the number of results would be in excess. Therefore, another selection of protocols is made based on their category. It is assumed that this selection step is justifiable, because the protocols in the same category use equal mechanisms for accessing the channel. The simulation setup is described in Section 2.4 and the performed simulations are described in Section 2.5.

2.1 Selection criteria

In the first stage of the project the available MAC protocols are listed. The protocols are collected from literature. The applicability of each protocol is investigated based on the scope of the project. A checklist is presented in Paragraph 2.1.1. These are objective requirements upon which the MAC protocols are selected. A description of these requirements is given in Section 2.1.1. The requirements are based on the following important capabilities which originate from the scope.

1. uplink

2. energy efficient

3. star topology or last hop

4. suitable for the scope of this project

These capabilities the MAC protocol can partly agree with, therefore strict requirements have to be set to make a good checklist. The strict requirements are first gathered in Section 2.1.1. From this a comprehensive list is created.

2.1.1 Definition of criteria

The selection based on these criteria is required to drop protocols which would have some clear drawback in any of the aforementioned capabilities or are not even capable to be supported in the scope of the project. At the end of this section a comprehensive list of criteria is presented, which is based on the arguments given here.

Uplink There are different types of packets that can be communicated by a transceiver. These can be data, preamble, acknowledgment, reservation, and so forth. Uplink means a packet containing data requires to be sent from a node to the sink. Setting the destination is not required, since in the uplink scenario the data packets can only be intended for the sink. Other message types can be sent from the sink to the node or even between nodes. All nodes in the network are assumed to be equal and generate the same load. Such a network is called homogeneous. In a homogeneous network each node has the same priority. Having the ability to prioritize certain packets in the MAC protocol is therefore considered unnecessary and will not contribute to better performance.

Star topology or last hop In this project MAC protocols are investigated which can be used for star topology. This means they do not need to include a routing mechanism. In a star topology the base station can be implemented with a power hungry transceiver reaching very high performance. In this situation the nodes can be made simpler. The energy efficiency of the network would gain from this. As a tradeoff exists between energy efficiency and base station power consumption, the MAC protocol energy efficiency will be optimal when no measures are taken to reduce power consumption in the base station. When a node decides to join a network this can be done in an autonomous or manual way. The preferred way is that the node discovers and joins the network autonomously, which means there should be a way of accessing the medium without being explicitly granted permission to do so. Many MAC protocols will have support for this, while others may need to implement support out-of-band.

Energy efficient Major energy consumption factors for nodes are (idle) listening, overhearing and (re)transmission. To improve the energy efficiency of the node, it is thus important to reduce these factors while maintaining a good QoS. What this effectively means is that nodes should not listen to messages meant for others, collision should be minimized and congestion of the channel should be prevented. When the node is scheduled to receive a packet, the rendezvous time for this schedule should be known beforehand at the node. This will allow the node to remain idle in the meantime. Nodes which have to listen all the time, because they do not know when the message arrives, waste energy in idle listening and overhearing. The transmission of packets other than data will not result in energy efficient behavior. This is due to the small data packets. Since data packets are almost the minimum required size, considering preamble, Identifier (ID), cyclic redundancy check (CRC) and data. Transmission of other packets, such as request to send (RTS) will not be considered energy efficient for UNB.

Suitable for the scope of the project As the type of physical layer and the MAC protocol performance are to a large extent independent of each other, the physical layer type does not have to be included in the comparison of the MAC protocol. This does not mean that nonidealities of the physical layer will not influence the MAC performance. The chosen implementation of the physical layer is based on the specifications of the Sigfox network, this means there are some limitations with respect to the options for MAC protocols. For instance BPSK does not permit the use of some medium access techniques. BPSK demodulation requires a coherent receiver and does not allow energy detection as receiving mechanism, since both ’0’ and ’1’ transmit the same power. When the modulation scheme relies on energy detection, like possibly in on-off keying (OOK) modulation, two signals sent at the same time may result in a logical OR behavior (if timed properly). Some MAC protocols use this behavior, so these protocols cannot be included in this project. Another technique that is used for MAC is CDMA. This has some variants but can be used to multiplex multiple transmissions on the same frequency with the use of orthogonal coding. With CDMA the required bandwidth is usually higher, due to a higher chipping rate. This would mean that either the signal is not UNB or the bitrate would drop dramatically resulting in unnescesary high energy consumption. Another issue with CDMA is the so called near-far problem [9], where power control is required to allow multiple signals to remain orthogonal and not overshadow each other. Power control is not feasible for low number of small packets per node, because of the varying channel characteristics and required overhead. The very low duty cycle and mobility of the sensor nodes makes it hard to keep up to date estimations of the channel load and characteristics. Protocols that rely on estimation to do adaptive medium access control will therefore not be considered for this project. Also in the scope of this project all nodes will start of as equals. No priority access is allowed for certain nodes.

List of criteria The criteria listed below in this section are strictly Boolean: they are either true or false. When a MAC protocol has these criteria satisfied it is able to be operated efficiently in the UNB network of this research.

1.1 MAC protocol is just intended for uplink.

2.1 The energy consumption in the receiver is not a concern.

2.2 Nodes should be able to know or predict the moment they are accessed.

3.1 Protocol does not have a mechanism for routing or forwarding.

3.2 No reservation packets should be used.

4.1 Nodes require to be able to do autonomous contention of time and frequency slots.

4.2 The network is homogeneous.

4.3 Protocol should be compatible with a basic PHY, which is capable of transceiving and clear channel assessment (CCA).

4.4 Protocol should not use load estimation at the nodes.

2.2 Model and assumptions

The model for comparing MAC protocols is based on the often used OSI based model as discussed in Chapter 1. In this research project each layer will have it's own implementation. The layers above the data link layer have a very basic implementation. In this project only the influence of the data link layer is investigated. The influence of physical and application layers is investigated by setting the corresponding parameters that will be given in sections 2.2.1 and 2.2.5.

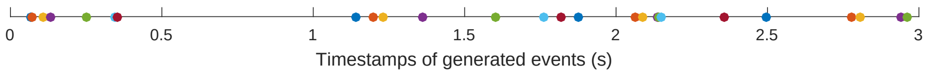

Figure 2.1: Events generated by a Poisson process with $\lambda = 0.1$

2.2.1 Application layer model

The applications for this project are modeled as packet generators at a certain average rate. Packets are created at application level and delegated to lower layers for transmission. At the sink the packets are directed back to the application layer. At the sink the processing and extraction of packet performance can be done. The number of successful packets and average delay of packets can for instance be calculated. The combined performance of single packets will in the end form network averages as FOMs. The packet generation process depends in general on many factors, of which the intended application is the most prominent. A simple and often used model for packet generation is the Poisson process.

Poisson process A Poisson process generates randomly timed events at a certain average rate. The process got its name from the Poisson distribution, which predicts the probability of n events happening in a certain timespan. The timing of each individual event is independent. The time between two consecutive events is exponentially distributed. In simulation the time instances at which events take place can therefore be generated by adding the numbers that are drawn from the exponential distribution, defined as

$$f(x) = \lambda e^{-\lambda x}. \tag{2.1}$$

In which, λ represents the average of the distribution. This corresponds to the average rate of the Poisson process. A sample stream of events, generated with the exponential distribution, is shown in Figure 2.1. The Poisson process is applied such that every generated event corresponds to a new packet at the application layer. One of the useful properties of a Poisson process is that multiple independently running processes have the same overall effect as a single Poisson process with its average rate divided by the number of processes. This means each node can generate its own events based on a Poisson process with an average rate of λ and the overall events generated by all nodes also behave as a Poisson process, with an average of $M \cdot \lambda$. This effective Poisson process of all nodes is associated with the network load. The relation between the network load and the average rate at each node is given by Equation 2.2, in which the network load is expressed in Erlangs.

$$\text{network load} = G = M \cdot \lambda \cdot L \cdot T \tag{2.2}$$

The number of nodes (M) and the duration of a packet transmission ($L \cdot T$) can be used to determine the average network load in Erlang. The Erlang unit is used to represent the channel usage. A network load of 1 Erlang is equivalent to a full channel; i.e. when packets are transmitted directly after each other the channel is occupied 100% of the time. A higher load than 1 Erlang is guaranteed to have collisions in a single channel. However, due to frequency multiplexing or the capture effect part of the generated load may still arrive correctly. This definition of network load is similar to the definition used by Abramson [10], with the difference of λ being per node generated load and the inclusion of retransmissions. This assumes retransmissions and arrivals combined are still a valid Poisson process, which is only valid when the time before retransmission is exponentially distributed and the time used for transmission is negligible. This assumption cannot be guaranteed for just any MAC protocol. The Poisson process is very convenient to use because it is so simple. However, it has its limitations. When the generation of events is spatially correlated the Poisson process does not produce a valid estimation for packet generation, because the simulated stream of events is supposed to be independent and irregular. For instance in a WSN that detects wildfire. In such a scenario it is likely that multiple nodes detect the same event at the same time. When the nodes start their transmission at the same time a collision is imminent. Other models have been invented to describe the time correlation. However, these are not part of this research.

2.2.2 Transport layer model

The transport layer model may ensure reliability of the network. The transport layer uses acknowledgment and retransmission with exponentially distributed back-off time. The transport layer retransmits the packet from the application layer to the network layer and the MAC state machine is reset. This happens when no acknowledgment has been received and the number of retransmissions has not exceeded the predefined limit. The transport layer waits before the next attempt. A flowchart of the transport layer process is presented in Figure 2.2. The intention of retransmission is to increase reliability of the link in unfortunate case of collision.

2.2.3 Network layer model

Since routing is not used in a star-topology-based network, the simplest possible network layer is used for simulation. This network layer forwards each generated packet to the sink, where the application packet is processed. No packets are generated at the sink. However, signaling packets such as acknowledgments and bea-

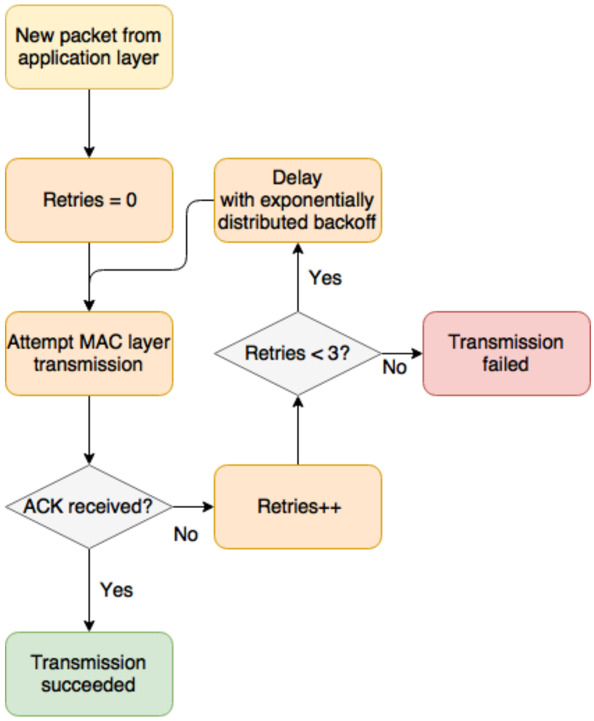

Figure 2.2: Flowchart of the transport layer with up to 3 retransmissions and exponential backoff.

cons use an out-of-band error-, delay- and collission-free channel as in agreement with the scope.

2.2.4 Data link layer model

The data link layer model is the actual implementation of the MAC protocol, as it would be in practice. MAC protocols behave according to a finite state machine, which can easily be implemented digitally without introducing approximations. However, some nonidealities of the digital system may affect performance. The most prominent is rendezvous mismatch due to limited time synchronization or oscillator accuracy. Many MAC protocols optimize the performance of a single channel and may multiplex many of those channels on the available bandwidth in such a way that they have very low adjacent channel interference. However, in UNB this approach will not suffice. Because of frequency uncertainty, being larger than the signal bandwidth, there may be multiple transmissions on the same channel without collision. It is expected that under the influence of relatively large frequency uncertainty, the optimal solution is to make use of partially overlapping channels. The way the partially overlapping channels influence the performance of the MAC protocol is found out by simulation of multiple channels in parallel with different channel separations. In this setup the channels are uniformly spread over the available bandwidth and the node chooses a random channel for any channel access. The base station is assumed to be listening on all frequencies and makes no distinction between channels.

2.2.5 Physical layer model

The physical layer gets its data delegated from the MAC layer. The physical layer is responsible for translation of bits in actual signals. This includes pulse shaping, modulation, demodulation, amplification, etc. The traditional approach is a collision model, which does not allow more than a single transmission in the channel. This model is, however, of very limited use for UNB. Due to capture effect there is a probability that one of the two or more frequency overlapping transmissions is received without error, instead of both packets being dropped. Because of frequency uncertainty there is even likely that two signals on the same channel do not overlap and are received correctly. The additive white Gaussian noise (AWGN) model is introduced to cope with partially overlapping channels and the capture effect.

Additive white Gaussian noise channel model Calculations on packet error rate (PER) are often based on signal to interference plus noise ratio (SINR), where the ratio between signal power and interference plus noise power is used to estimate the average bit error probability of a receiver. In this model it is assumed that wideband interference sources, such as orthogonal frequency division multiplexing (OFDM) networks, give rise to an interference contribution approximated with AWGN. Other noise contributions come from interference of UNB transmissions and noise. Modeling interference as AWGN is an approximation which only gives valid estimations when many interference sources are present. This is a result of the central limit theorem [11]. The central limit theorem shows that addition of many stochastic variables will result in a Gaussian distribution. This does not hold for inter symbol interference (ISI), since the effect of self made interference can be very different and depends on other factors. With a proper choice of pulse shaping filter the distortion caused by ISI can be reduced to a negligible effect. Such a pulse shaping filter is an root raised cosine (RRC) filter, which is used in this model. The pulse shaping filter spreads the power over both time and frequency, to lower the signal bandwidth, reduce ISI and limit fast fluctuations in power consumption. A representation of a general modulation scheme can be seen in Figure 2.3. The most simple version of this model assumes a steady center frequency, perfect pulse shaping, perfect synchronization and no phase noise. The total SINR, modeled as AWGN, can be calculated for any pulse shaping filter setup. The interference as a function of frequency difference between the interferer and the source is called the rejection coefficient [6] and is denoted with β. In our setup the rejection coefficient is just a

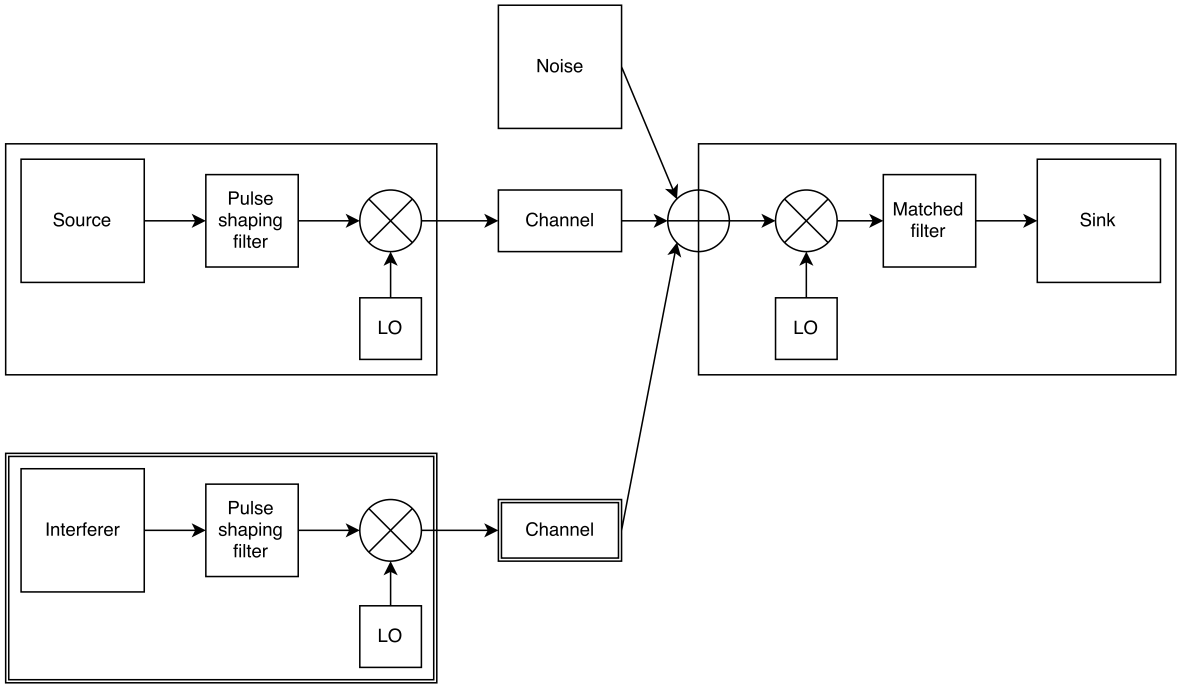

Figure 2.3: Block diagram of physical layer model

function of frequency separation (δ_ω) as seen in the equation below.

$$\beta(\delta_\omega) = \frac{\Big\{(p_t(-\tau) * p_t(\tau)) \cdot \cos(\delta_\omega \tau)\Big\} * p_r(-\tau) * p_r(\tau)\Big|_{\tau=0}}{2T\Big\{p_t(\tau) * p_t(\tau)\Big\}^2_{\tau=0}} \tag{2.3}$$

The rejection coefficient can be calculated for a given pulse shaping filter with impulse response $p_t(\tau)$, matched filter with impulse response $p_r(\tau)$ and symbol duration (T). A derivation for the AWGN contributions can be found in Appendix A. Noise in the system is modeled as a AWGN with a power level of N_0. The noise power that remains after the matched filter is the noise coefficient. The effect of this is denoted with γ and is calculated as

$$\gamma(N_0, P_x) = \frac{N_0\Big\{p_r(-\tau) * p_r(\tau)\Big\}_{\tau=0} \cdot \Big\{p_t(-\tau) * p_t(\tau)\Big\}_{\tau=0}}{2TP_x\Big\{p_t(\tau) * p_t(\tau)\Big\}^2_{\tau=0}}. \tag{2.4}$$

In this equation the noise contribution to the SINR can be found, as a function of transmit power (P_x), pulse shaping filter impulse response ($p_t(\tau)$), matched filter impulse response ($p_r(\tau)$), symbol duration (T) and noise level (N_0). As the rejection coefficient is for a single interferer. For the total SINR the rejection coefficient has to be multiplied by the number of interferers. All interferers have their own frequency difference and may therefore have different interference strengths from the rejection coefficient. In our model the frequency difference comes from two sources, i.e. it has been applied intentionally by the transceiver and an unknown factor is caused by frequency uncertainty. In the model used here SINR is built up from the three different sources of Figure 2.3, i.e. the intended signal, the interfering signals and the background noise. The signal, interference and noise will result in a varying SINR and therefore a varying bit error rate (BER). The time varying BER is a function of the rejection coefficient, the individual interferers and the noise, as given in Equation 2.5.

$$BER(t) = \frac{1}{2}\mathrm{erfc}\left(\sqrt{\left(2 \cdot (\sum_{k=1}^{K(t)} \beta(\delta_{\omega,k}) + \gamma)\right)^{-1}}\right) \tag{2.5}$$

The BER depends on the number of simultaneous interferers (K) with each a different frequency offset $\delta_{\omega,k}$ and the noise coefficient (γ). The probability for a bit error of bit n depends on the BER at the time of sampling (t_n). The SINR can thus be converted in a BER and this is equivalent to the probability of a bit error for a single bit. The probability that a wrong decision is taken at the sampling time corresponds to the BER value at the sampling instant. L number of contiguous bits form a packet, in which each bit can be erroneous. The PER is equal to the probability that a certain packet has one or more bit errors and is calculated as follows.

$$P(\text{packet error}) = 1 - \prod_{n=0}^{L-1}(1 - P(\text{bit error of bit n})) \tag{2.6}$$

The PER may be improved by including forward error correction (FEC), the correction will come at the cost of additional bits but may help to recover packets with a few bit errors. Figure 2.4 shows the PER as a function of signal to interference ratio (SIR) and the number of bits that have been under the influence of an interfering signal. If two packets are transmitted at the same time, an SIR of approximately 7 dB is required to have 10% capture probability. The interfering packet will then probably be lost. If 20 bits of an interfering signal arrive at equal strength as the intended packet, both packets have 80% probability of being lost. It can be noted from the graph that a high SIR value gives low probability for packet error. Increasing the time an interferer will also increase the probability of packet errors.

Frequency uncertainty Frequency uncertainty is present in any local oscillator. It means the frequency of oscillation cannot be accurately determined. Crystal oscillators in combination with phase locked loops (PLLs) are most often used for generating a signal with the specified RF frequency. These crystal oscillators come in a variety of specifications. A tradeoff exists between cost, size, power consumption and accuracy. Therefore very accurate frequencies are not feasible for wireless sensor nodes, since WSN require nodes to be low in cost, size and power consumption. In a UNB system the signal bandwidth is much less than the uncertainty of the center

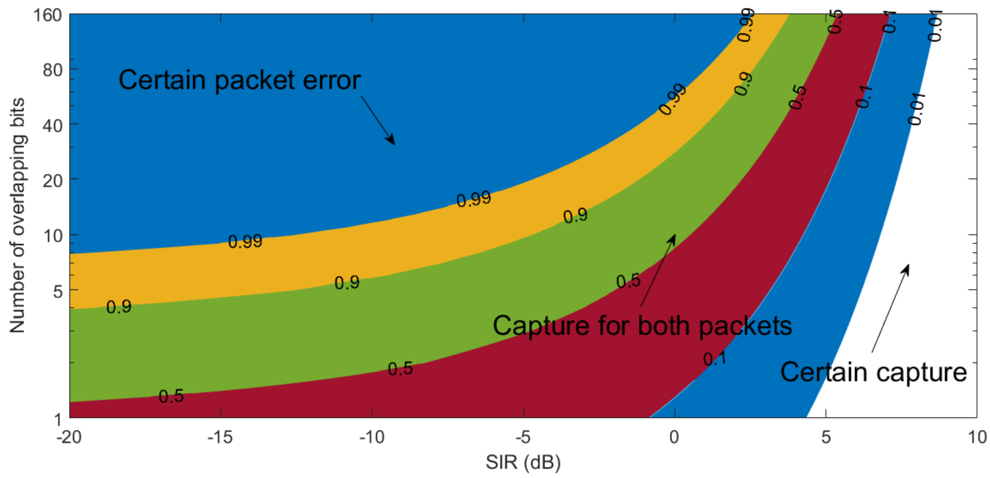

Figure 2.4: PER performance as function of overlapping bits (L' out of 160 bits) and SIR without noise.

frequency resulting in the following situation. Because of the frequency uncertainty, two or more signals intended to be transmitted at the same center frequency may end up being frequency multiplexed, in which case the base station may be able to receive all of them. In such a situation the packet delivery ratio (PDR) is much higher than expected based on the single channel assumption. Frequency uncertainty should therefore be modeled to retrieve valid FOMs for UNB communication systems. Frequency uncertainty of a crystal is specified by the supplier as a value in ppm. The ppm value corresponds to the maximum expected frequency difference from the nominal frequency. After multiplication by the PLL a 10 ppm oscillator at 868 MHz, may vary between 867.99132 and 868.00868 MHz. To model this, the frequency deviation is randomly picked from a Gaussian distribution [6], with $\mu = 0$ and $3\sigma =$ Frequency uncertainty defined in ppm. This ensures 99.7% of the samples δ_f taken from the distribution are within the specified uncertainty range of the oscillator. The actual frequency the node is calculated as follows,

$$f_{node} = f_{intended} \cdot (1 + \delta_f * 10^{-6}) \tag{2.7}$$

Time uncertainty Like frequency uncertainty, time uncertainty comes from the uncertainty of an oscillator. This oscillator is used to keep track of time. A difference in oscillation frequency makes the local time run slower or faster than that of the base station or that of another node. This may cause problems when a rendezvous appointment has been made, but the clocks drift apart. Like frequency uncertainty, time uncertainty is specified in ppm. In case of a 100 ppm crystal oscillator, after 1 day the clocks of unsynchronized nodes in the system may have drifted off ±8.64 seconds. The conventional way in a time slotted system to prevent collisions because of time uncertainty is to add guard times between the time slots. Having too long guard times leave the channel unused and causes performance to go down. In UNB systems the time uncertainty will not cause bad performance. Because of the long transmission time for a packet in UNB, the guard time is just a fraction of the total slot time. Even when synchronizing every 100 seconds, having a 100-ppm crystal and 50 time slots, a guard time of 0.01 seconds suffices. This is only 0.5% of the total time. When applying slotted time systems in UNB a small guard time can be used to prevent collision because of time uncertainty. It is therefore not required to model time uncertainty as the expected effect is negligible.

Frequency drift Because the packet transmissions in UNB may take such a long time it may very well be that the frequency of transmission drifts off while transmitting. For frequency drift two causes can play a role. The first is Doppler effect due to acceleration, as described in [12]. The second is environmental changes that influence oscillator frequency. Frequency drift due to Doppler effect is very small for a system with a static base station. Acceleration above 10G are not expected, while this results in a frequency drift of only 2.9 Hz/s. The maximum expected frequency drift over a packet duration of 1.6 seconds is then only 4.6 Hz. Compared to the 100 Hz signal bandwidth this effect is negligible. The environmental changes are not expected to have a very high influence. Temperature, pressure, humidity or stress are not expected to change very rapidly, therefore the short term drift of frequency can be neglected. On a longer term the frequency can change. When generating only a few packets per day the frequency of access will be uncorrelated. In this model the frequency drift is neglected, this means that the frequency of any node will not change in the course of simulation.

Phase noise Phase noise is present in any oscillator. It can be described as short term random fluctuations in the phase of the local oscillator (LO). Phase noise is thus present in both the transmitter (node) and the receiver (base station). By using more power the phase noise can be reduced, therefore phase noise in the base station can be neglected. For the transmission of a uplink packet the only relevant contribution of phase noise is the noise generated at the nodes LO. Whether the phase noise is generated at the transmitter or the receiver does not matter, as depicted in [13]. This in combination with the phase noise performance for slow BPSK as presented in [14], show that phase noise can influence BER in our system. This research won't include a model of phase noise. However, as it might have an influence it will be interesting to investigate in further research.

Path loss One of the major motivations for this research is the expectation that CSMA performs better than Aloha in a UNB communication system. One of the major drawbacks of CSMA in UNB is the hidden node problem. This is because sensing the channel before transmissions will only increase performance when the business of the channel can be detected reliably. When nodes are too far away to sense each others ongoing transmission a collision occurs. In this research the path loss is modeled as

$$L_P = \frac{P_r}{P_t} = K\frac{d_0}{d}^{\gamma} \tag{2.8}$$

, as explained in [15] section 2.5. In this equation K is a constant representing the path loss at reference distance d_0, γ is the path loss exponent and d is the distance. In general this model estimates the average effect of distance with exponent γ on the power received by an antenna. In this model γ depends on the environment and K on the frequency of operation. Typical values of γ range between 2 and 4. For this research a value of 3 has been chosen.

In simulation the path loss is determined from the random positioning of the nodes. In this research the nodes are assumed to be uniformly distributed over the area within range of the base station. The sensitivity, transmit power and the path loss exponent are required to determine the range of the base station. A value of -142 dBm is taken as receiver sensitivity of the base station. This value corresponds to the sensitivity of the base station in a Sigfox network [4]. The range that can be achieved with a system operating in the 868-MHz band with a transmit power of 10 dBm is roughly 10 km. The average number of nodes per square meter can be calculated as

$$\text{Average number of nodes per m}^2 = \frac{M}{\pi d_m^2} \tag{2.9}$$

With M the number of nodes in the network and d_m the maximum distance to the base station in meters. The nodes are placed in simulation using a triangular distribution for the range and a uniform distribution for the angle. This way the nodes will have a higher probability of being placed far away from the base station. This observation results in a relatively high probability of having hidden nodes, since the distance between nodes is large.

Fading Fading as described in [15] is a stochastic process that extends the path loss model. There is a difference between small scale and large scale fading. In addition to hidden nodes problem, in a fading channel nodes may be hidden for the base station despite being in its range. Signals in an UNB system will experience frequency flat fading, because of the very small signal bandwidth. However, because of the long packet lengths the fading may occur while transmitting a packet. When the coherence time of a certain environment is below the packet transmission time, the PER is higher. In this research the effect of fading is not investigated. However, as described above it will be interesting to investigate the performance of UNB in a channel if average non-fade duration is shorter than the packet length.

2.3 Figures of merit

After a list of MAC layer protocols is created and suitable protocols are selected, it will be time to get some quantitative results from the protocols. The goal is to find the best fit for different operating conditions by comparing the FOMs. The FOMs give important insight in the performance of the MAC protocols. Due to previously given limitations of the model the FOMs may not be achievable in a real scenario.

2.3.1 Packet delivery ratio

PDR is a FOM that gives insight in the reliability of the network. There will always be a possibility that generated packets are lost in the delivery process. This may be due to signal propagation loss, collision, fading dips, congestion in the channel, or any other reason. Packet delivery ratio and its counterpart packet loss probability, or packet drop ratio, are common metrics for capturing WSNs performance. The ratio is calculated as follows [16]

$$\mathrm{PDR} = \frac{\sum \text{received packets}}{\sum \text{generated packets}} \tag{2.10}$$

In a simulation the PDR achieves its steady state result after some time. PDR will be a value between 0 and 1. A value of 1 means every packet has been delivered successfully. Applications will require a high enough reliability of the link to limit communication errors. This is achieved by having a certain PDR. In this research an arbitrary value of 90% has been chosen. To improve packet delivery ratio there are several options, one of which is to do retransmission after failure. Where this helps to increase packet delivery ratio in noise limited transmission or fading dips, in a congested channel retransmissions will make it worse. The MAC protocol is responsible to prevent congestion. MAC protocols which do prevent congestion effectively are expected to have a higher PDR in high load situations.

2.3.2 Throughput

The conventional approach to measure network performance for MAC layer protocols is throughput. Many different definitions can be found. We have chosen to represent throughput as the succesful part of the network load, and network load as the ratio of channel usage when packets are perfectly scheduled. The definition is

$$S = \mathrm{PDR} \cdot G = \mathrm{PDR} \cdot M \cdot \lambda \cdot L \cdot T \tag{2.11}$$

, where G is the network load, M the number of nodes, L packet length and T symbol duration. This is in accordance with the definition proposed in [10].

The throughput versus network load graph is often seen in MAC protocol research such as Aloha or CSMA as given in [7]. The definitions of network load and throughput have been chosen to coincide with the definitions shown in this paper. The resulting performance from simulations in this thesis can thus be directly compared to these results. Throughput is always less than the network load. A perfect MAC would increase throughput along with network load until both have value 1. Throughput should not increase beyond this point. However, due to the capture effect and frequency multiplexing the throughput can go up even further. The throughput can be interpreted as the average number of successful transmitted packets on the channel within the observation time. The maximum throughput depends on the ability to frequency multiplex and the ability to reject interference at the base station and to capture the incoming packets.

2.3.3 Network fairness

To measure whether the resources, i.e. the available spectrum, is divided equally between the nodes in the network a measure of fairness is considered. Their are several different definitions to sense the fairness in a wireless network. Jain et al. [17] propose the so called Jain fairness. This metric is supposed to be independent of the population size (number of nodes). The Jain fairness is both a bounded and a continuous measure of fairness. In wireless networking Jain fairness is calculated on average throughput or average delay per node. Since reduction of delay is not the main design criterion for WSN the throughput has been chosen. Other interesting fairness metrics would be the fairness of energy consumption per node. This will make it possible to calculate the battery lifetime expectancy of a node with more certainty. Moreover, a high energy consumption fairness will reduce outage probability in an energy harvesting scenario. We will be considering only Jain fairness on average throughput per node [18]. Jain fairness can be calculated using Equation 2.12,

$$F_J = \frac{S^2}{M \sum_{i=1}^{M} S_i^2} \tag{2.12}$$

, where S_i is the throughput for node i, M is the number of nodes and S is the throughput of the whole network. This FOM gives a measure for fairness of the usage of the available spectrum and is more applicable for the design of the network. When designing node architecture it may be important to find the fairness in energy consumption. Jain fairness is bounded between 0 and 1. A value of 1 resembles a fair network, where every node has the same probability of delivering its packets to the base station. The distance to the base station is one of the parameters that have large influence on the fairness, because nodes nearby the base station are able to have its packets received with much more power than nodes at the edge of the base station range.

2.3.4 Energy consumption

Energy consumption is, as clarified earlier, one of the major challenges in WSNs. Furthermore, especially the MAC protocol has large impact on the lifetime expectancy of a node. An estimation of energy consumption of nodes in a WSN can be found in [19]. Unfortunately the power consumption of the nonexistent hardware is unknown, so most of the parameters described here cannot be filled in. To circumvent this, a good measure is to capture the average time that the wireless transceiver is on per packet. Energy consumption can roughly be divided into transmission and reception energy, as given in the following equations

$$E_{tx} = T_{start}P_{start} + \frac{n}{RR_{code}}(P_{txElec} + P_{amp}) \tag{2.13}$$

$$E_{rcvd} = T_{start}P_{start} + \frac{n}{RR_{code}}P_{rxElec} + nE_{decBit} \tag{2.14}$$

The energy required for transmission requires a start up of the oscillator and amplifier, this is resembled with the time required for startup (T_{start}) and the power consumption during startup (P_{start}). After the startup has been completed the packet can be transmitted. The energy budget required for this is the packet transmission time ($\frac{n}{RR_{code}}$) and the power used during transmission (P_{txElec}). In receive mode the power for startup and receiving (P_{rxElec}) is equal to that of transmission mode. However, the receiving part as additional power consumption in the energy required to decode the packet (E_{decBit}). The startup phase can be neglected because the packet transmission time and power used during transmission is much higher than the time and power used for startup. A packet in UNB can easily take 2 seconds, while the startup takes around 100 microseconds. According to datasheet of a Sigfox transceiver, the energy required to receive a packet is much smaller than the energy required for transmission [20]. This can be attributed to both higher bitrate, meaning the receiver has to be on only one sixth of the time of the transmitter, and the current consumption in transmit mode, which is three times higher than in receive mode. The same argument applies to the sensing of the channel, which takes only a very short time to complete. It can therefore be concluded that energy consumption is determined mainly by the transmissions of the node. Given consumption during transmission is the main source of energy consumption in a node and the fact that energy is the time integral of power, the total time a node spends in transmission is linearly related to the energy consumption. Keeping track of the time spent in transmission state is therefore a valid FOM to measure energy efficiency. The energy efficiency is then defined as

$$\epsilon = \frac{\text{Useful energy spent}}{\text{All energy spent}} = \frac{\text{PDR} \cdot T \cdot L}{\text{average time transmitting per packet}} \tag{2.15}$$

Retransmissions will cost energy, which would halve the energy efficiency. Preventing retransmissions by doing CCA and reducing collisions is essential for energy efficient MAC protocol operation. A value of 1 would mean the least possible energy is consumed for transmission. Lower values would mean more energy is consumed to transmit a packet or energy is wasted on lost packets.

2.3.5 End-to-end delay

Some applications, such as alarms or control systems, require predictable and low delay to function appropriately [21]. While in this project the delay is not of importance the delay introduced at the MAC layer is not a significant design criterion. In communication systems the delay of a packet is at least the packet transmission time, which is quite high for UNB. Retransmission strategy, beacon interval, contention mechanism and other MAC protocol techniques have an impact on the average time until successful packet delivery. The definition of end-to-end delay is shown in below and has been taken from [16].

$$D = \frac{\sum_{i=1}^{N_{packets}} (t_{success,i} - t_{creation,i})}{N_{packets}} \tag{2.16}$$

The average delay (D) is calculated from the number of received packets ($N_{packets}$) and the delay of those packets ($t_{success,i} - t_{creation,i}$). The definition only considers successful packets because it is the most convenient to know how long a packet will take before it is delivered. The lifetime of an unsuccessful packet is not considered and is not important.

2.4 Simulation setup

Simulation is performed using OMNeT++ 5 simulator [22]. Other simulators are not up to the task of including at least frequency uncertainty. Castalia is a simulator based on OMNeT++ that comes close to the required features. However, it requires serious adjustments to be made before it could be used for this research. This means a new framework for simulations in OMNeT++ has to be created. It requires that all subsystems are implemented as in the model presented in Section 2.2. The network in OMNeT++ exists of a number of nodes, which each have an application, MAC protocol implementation and PHY layer implementation to generate packets and transmit the packets at the right time and frequency. The nodes are connected using a channel module, which is responsible for keeping track of all ongoing transmissions, the calculation of packet errors and the delivery of packets to the base station.

2.4.1 Nodes

A node consists of an application, MAC protocol and PHY layer. The applications keeps generating packets at a specific offered load as a Poisson process. The offered load at which the packets are generated is the network load G divided by the number of nodes M. If the MAC protocol is still busy with the transmission of a previous packet the current packet is dropped, this is called the zero buffer assumption. By increasing the number of nodes the probability of having an initially dropped packet becomes very low. It can be so low that the infinite node assumption becomes approximately valid. In simulations the network load is incremented until no further load is required. The load is increased by increasing the offered load per node (λ). This means the number of nodes is fixed for all simulations in that series. This also means that at high offered loads per node and with a high delay the initial rejection of packets may increase. When that happens the infinite node assumption is not valid anymore. In the simulation framework the nodes are created at startup. This means the positions and the frequency uncertainty do not change during a simulation. This may cause bad accuracy when the number of nodes is low. This effect can be countered by doing multiple repetitions of the same simulation and average the results if required. CSMA like MAC protocols require the possibility to sense the channel before transmission. This is also called CCA. This is done with the same physical layer as for transmission. The received power is integrated over one bit duration to find the RSSI. When the collected energy is higher than a certain value the channel is considered busy and transmission is postponed.

2.4.2 Simulation framework verification

To present evidence of the validity of the simulator a couple of simulations are done. The throughput is the most common FOM for MAC protocol performance. For many

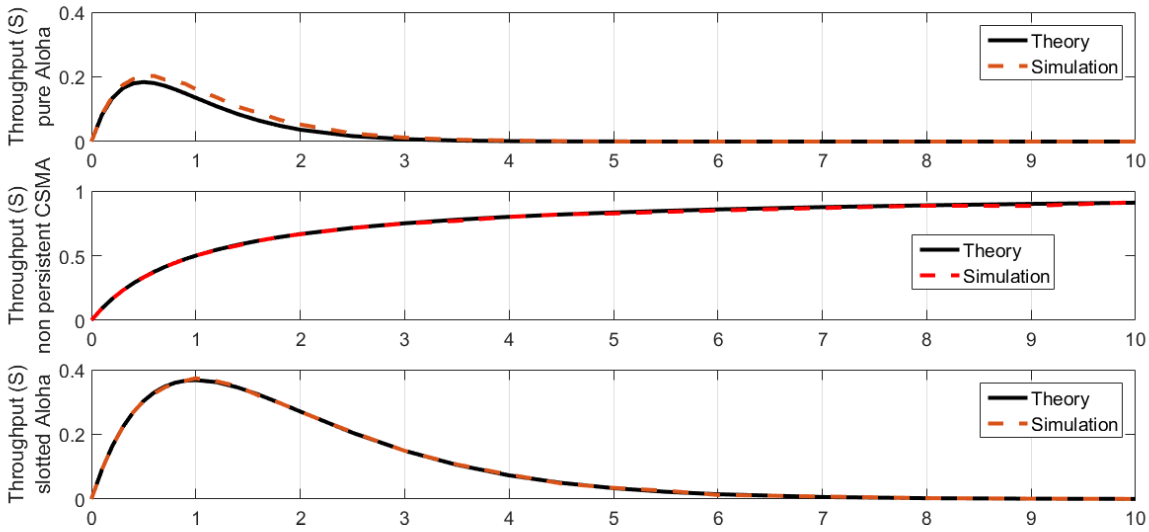

Figure 2.5: Comparison of theoretic and simulated throughput for pure Aloha, slotted Aloha and non persistent CSMA.

basic MAC protocols the throughput can analytically be predicted. Pure Aloha, Slotted Aloha and non persistent CSMA are a couple of protocols that have well known throughput:

$$\begin{aligned} S_{\text{pure Aloha}} &= Ge^{-2G} \\ S_{\text{slotted Aloha}} &= Ge^{-G} \\ S_{\text{non persistent CSMA}} &= \frac{G}{G+1} \end{aligned} \tag{2.17}$$

This throughput is valid under the assumption of infinite nodes (zero buffer), zero propagation delay, Poisson generated network load, no hidden nodes, single channel and no capture effect. A simulation environment is setup that approximates these assumptions. The number of retransmissions is put to zero. All nodes are placed with equal distance to the base station, which corresponds to zero path loss. There will be 5000 nodes in the simulation. This will approximate the infinite node assumption when delay is small and packet generation rate is low as nearly all nodes will be done before a new packet arrives. The results of these simulations are presented in Figure 2.5 and plotted together with the throughput of Equation 2.17. No significant differences can be noticed between the expected and simulated graphs. This confirms the validity of the simulation framework to a certain extend. It does even show that the sensing mechanism works appropriately. In the single and multi channel simulations there will be some additional influence of the path loss and of retransmissions. In Figure 2.6 the effect of path loss and 3 retransmissions can be seen. There are a couple of observations that can be noticed as a difference between the simulations with and without path loss and by including retransmissions.

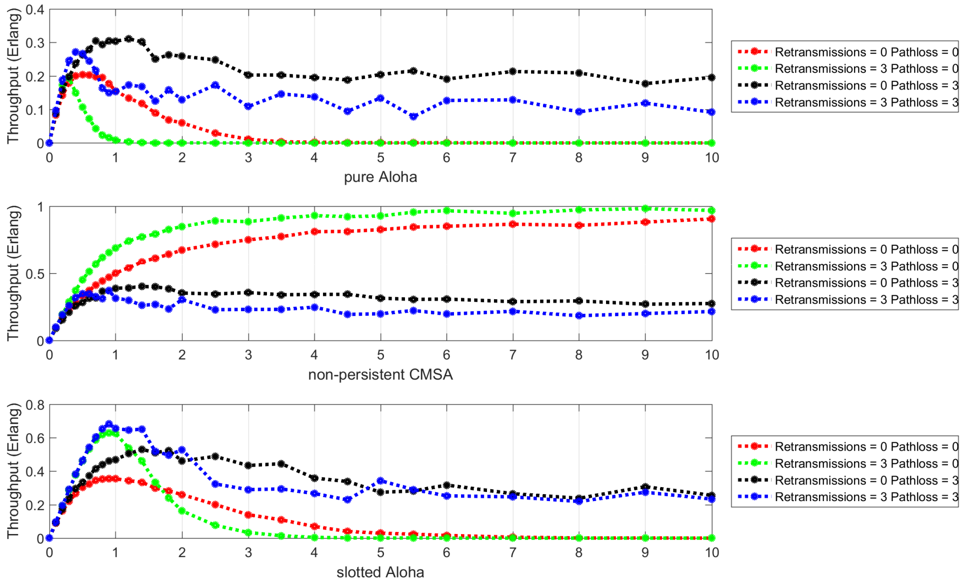

Figure 2.6: Comparison of simulated throughput for pure Aloha, slotted Aloha and non-persistent CSMA under the influence of path loss and retransmissions.

Throughput seems to be asymptotic if network load increases The throughput has an asymptotic behavior. In these regions the PDR drops at the same pace as the network load rises. This can be explained as a combined result of the uniform distribution of nodes over the area and no power control. The capture effect causes that only the nearest nodes take part in the delivery process, i.e. the nearest nodes will have the strongest signal. The packets delivered come from a relatively small part of the nodes that are positioned near the base station, the range at which nodes are able to deliver their packets successfully becomes shorter and shorter with increasing network load.

Throughput curve is not very smooth The results of simulation are based on a single set of random numbers from the random number generators. The accuracy of the position and frequency deviation of the nodes is limited by the number of nodes. This is because those parameters are setup only once at the start of simulation. Especially in the regions of high network load this results in low accuracy of the FOMs, because the number of nodes that affect the MAC protocol performance becomes lower as indicated before with the capture effect. However, each simulation is independent which means the trend should be obtainable.

Performance of Aloha with path loss is generally higher than without path loss Aloha is a just transmit kind of protocol. In the case of zero path loss, both packets are received with equal power, a collision will result in the loss of both packets. When path loss is included the packets arrive with a difference in received power. One of the transmitted packets will have a good chance of being delivered successfully. This results in a higher overall throughput, compared to when no packet has the probability that it arrives free of error.

CSMA performance with path loss is worse than without path loss Sensing the medium has two possible outcomes, it can be either idle or busy and the sensing mechanism can mistake idle for busy and the other way around. Because of the model used here only the average power is measured for sensing the medium. This means the outcome of CCA cannot be busy when it is actually idle. This situation corresponds to the exposed node situation. However, it is possible to measure an idle channel while it is actually free. This happens when the interfering node is further away than the range of CCA. CSMA performance is decreased by those hidden nodes. If all nodes would be hidden CSMA becomes equal to pure Aloha.

Due to retransmissions throughput decreases at high network load Because packets that do not arrive are treated as new arrived packets the effect of retransmission can be approximated as an increase of effective network load. At low load the channel may not be completely busy, so there is a chance that a retransmitted packet is delivered correctly after the retry. However, in a busy channel a retransmitted packet causes imminent collision and will lead to lower throughput. It can be concluded that retransmission in this form is effective, because without any form of frequency multiplexing the maximum operable network load is 1.

2.5 Simulations

Using the simulator described in Section 2.4 the best suitable MAC protocols, which are selected as described in Section 2.1, are considered for simulation. After the MAC protocol is implemented in the framework the simulations can be carried out. Some protocols may be assuming to spread the signal over a certain bandwidth, like the continuous random frequency division multiple access (CR-FDMA) protocols suggested in [6]. These type of protocols will be referred to as multi channel protocols. Protocols of this type use a frequency range instead of a single frequency. Conventional MAC protocols are single channel, and they are not designed for significant inter channel interference. The throughput that could be achieved in multi channel protocols is the number of channels times the throughput of a single channel. However, because of inter channel interference this will either not be efficient in terms of spectrum usage or the total throughput will be lower. Comparing single channel with multi channel protocols in a fair manner is a challenging task, because multi channel protocols cannot be converted into single channel protocols. However, the other way around is true. In simulation this is done by placing channels next to each other in frequency domain. Because of frequency uncertainty, the channels may have significant overlap, but this is accounted for by changing the channel separation accordingly. In the limit of number of channels going to infinity, the multi channel protocol becomes a CR-FDMA protocol. It may be possible that reducing the number of channels, thus increasing the separation, will have a positive effect on the performance of a certain protocol. However, if the protocol performs best at high number of channels, the CR-FDMA variant will be the more optimal solution for that MAC protocol. The distribution of center frequencies in a multi channel MAC protocol, subject to frequency uncertainty, is shown in Figure 2.7. Because of the infinite character of the Gaussian distribution it will not be possible to prevent any node from sending outside the intended bandwidth. The separation of the channels is tuned such that for a given number of channels the spillover of the overall frequency distribution is 5%. As the number of channels is increased the distribution of the center frequency becomes more and more uniform. It is expected that this uniform distribution, which corresponds to the CR-FDMA protocols, is the optimal solution for frequency multiplexing in UNB. The multi channel counterparts of Pure Aloha or Slotted Aloha are the ones described and proposed by [23], namely frequency unslotted time unslotted Aloha (FU-TU-Aloha) and frequency unslotted time slotted Aloha (FU-TS-Aloha). frequency slotted time unslotted Aloha (FS-TU-Aloha) and frequency slotted time slotted Aloha (FS-TS-Aloha) are frequency slotted versions, so they have a non-uniform distribution for center frequency like shown in Figure 2.7. These protocols are expected to have worse performance than the unslotted versions. Each simulation run consists of a number of nodes with random fixed position and frequency deviation. The number of nodes is chosen such that a representative simulation is achieved. Because of the no buffering assumption, there will be initial rejections of packets when the MAC protocol is busy with the previous packet. The parameters of the MAC protocols and network parameters are the same in all simulations. The chosen values are defined in Table 2.1.

The parameters such as the number of retransmissions, base station sensitivity, symbol duration, packet length and arrival rate are the same as in the Sigfox network [4]. The beacon rate is chosen equal to the arrival rate. The CCA parameters are chosen such that a node has equal range as the base station with a delay equal to a single bit duration. Transmission power and center frequency are chosen such

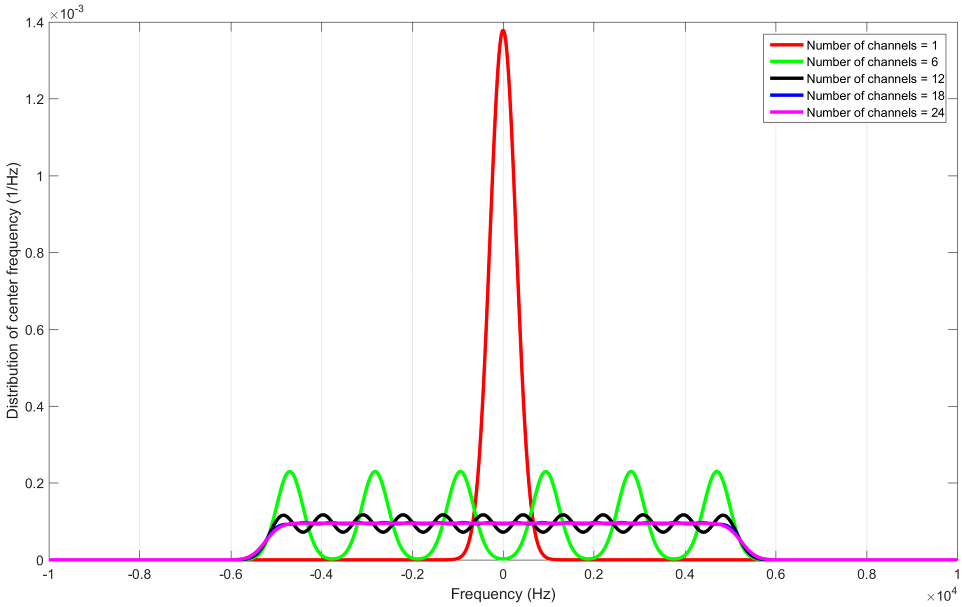

(a) A 1-ppm crystal reference in 868-MHz band distributed within 10 kHz bandwidth.

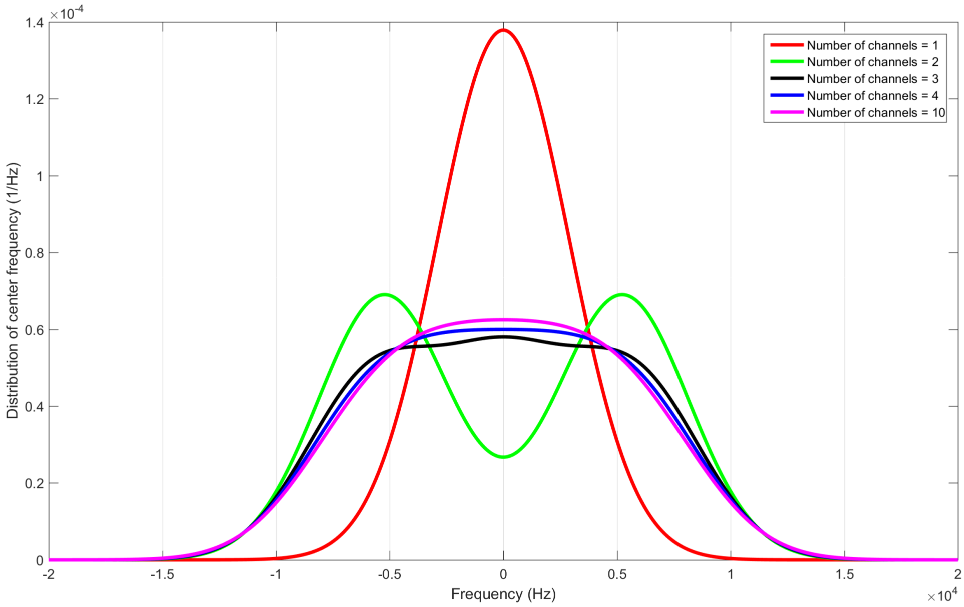

(b) A 10-ppm crystal reference in 868-MHz band distributed within 20 kHz bandwidth.

Figure 2.7: Distribution of center frequencies for the case of a multi channel MAC protocol. Separated by the number of channels with a maximum of 5% spillover outside the bandwidth.

Simulation parameters

Parameter	Value
arrival rate per node (λ)	100 packets/day
packet length (L)	160 bits
symbol duration (T)	10 ms
transmission power (P_x)	14 dBm
center frequency (f_0)	868 MHz
base station sensitivity	-142 dBm
path loss exponent	3
noise floor (N_0)	-174 dBm/Hz
CCA measurement delay	10 ms
CCA busy threshold	6.3096e-20 J
retransmissions	3
average time before retransmission (exponential)	10 s
slotted time guard	34.56 ms
beacon interval	100 beacons/day
multi channel bandwidth (1 ppm)	10 kHz
multi channel bandwidth (10 ppm)	20 kHz

Table 2.1: Simulation parameters for single and multi channel simulation.

that they do not violate regulations of the 868-MHz band. The bandwidth is chosen such that the simulations will be feasible. The guard time between slots is chosen such that worst case clock skew (with a 10-ppm crystal) will not result in collisions as in [24].

2.5.1 Single channel simulation

Single channel simulation will be done on all single channel MAC protocols that come through the selection procedure described in Section 2.1. It is assumed that all single channel MAC protocols, transformed into a multi channel protocol will have similar improvements. This is because all MAC protocols of a category use the same technique for medium access. If there is a reason to suspect a MAC protocol being different from others, a new category can be introduced. The single channel MAC protocols will be judged based on a smaller set of FOMs, namely PDR, throughput (S) and energy efficiency (ϵ). One of the basic constraints of having a working system is to have a good PDR. The minimum PDR to have a good communication system for this work is set to 90%, and the corresponding offered network load G_0 is given as in

$$G_0 = G(\mathrm{PDR} = 0.9) \tag{2.18}$$

The PDR is expected to be monotonically decreasing from 1 to 0 with increasing network load. Therefore, the selection of 90% will always result in a single intersection. Within each category the throughput and energy efficiency are taken at the network load (G_0) where PDR is 90%, then normalized to the maximum of that category and summed to retrieve the final score, as in

$$\mathrm{score} = \frac{S(G_0)}{\max S_c} + \frac{\epsilon(G_0)}{\max \epsilon_c} \tag{2.19}$$

This score is relative to each category. It basically scores the relative improvements of throughput and energy efficiency compared to other protocols in the category. The MAC protocol within each category with the highest score is selected for multi channel simulation. It is assumed that the unselected MAC protocols, which perform poorly in single channel simulations, would not outperform the other MAC protocols of that category in multi channel simulations. Therefore, by following this approach, the multi channel simulations, that would produce uninteresting results, are avoided.

2.5.2 Multi channel simulation

For multi channel comparison the number of channels are adapted in a series of simulations. In multi channel simulation each node selects a new random channel before each transmission or retransmission. The selection of the channel is based on a uniform discrete distribution. If the MAC protocol supports scheduling in the base station it will be able to divide the available slots in a optimal manner, i.e. the frequency slots are spaced as far away as possible. The number of channels are selected based on the frequency uncertainty. When frequency uncertainty is large (10 ppm), the number of channels can be very low to transform the single channel into its infinite multi channel counterpart. The multi channel FOMs can be compared with other MAC protocols or with another number of channels. The number of channels that show the best performance, based on the score, are compared to the other MAC protocols. This results in a comparison of the best MAC protocols, with the optimized channel separation for each MAC protocol category.

Chapter 3

Results

In this chapter the results of the tests and simulations are presented. This is performed along the method described in Chapter 2. The chapter starts with a selection of the protocols that are included into the project. Then the single channel protocols will be compared and selected in Section 3.2. In Section 3.3 the multi channel simulation is performed and the resulting FOMs for the protocols are presented.

3.1 MAC protocol selection

In Table 3.1 the results from protocol selection are shown. Only some of the best fitted protocols are shown, since the list would otherwise be too long. The protocols which do not satisfy the requirements are given in Appendix B.

Each of the protocols belong to a certain category and may have multi channel capabilities. The selection and categorization can be seen in Table 3.2.

3.2 Single channel simulation

For single channel simulation the MAC protocols from Table 3.2 are implemented and put to the test. Only the single channel protocols from the table are used for single channel comparison. The other MAC protocols are simulated in multi channel simulation and compared with multi channel variants of the single channel protocols. SIFT is a protocol that is expected to outperform other types of persistent CSMA protocols, because of its supposed optimized contention strategy. The resulting scores, as defined in Equation 2.19, are given in Table 3.3.

The MAC protocols with the highest score in the single channel simulations are selected to be simulated in a multi channel simulation. These MAC protocols are Slotted Aloha, non persistent CSMA and ISMA. However, because multi channel transformation will not give a practical solution for idle sense multiple access (ISMA)

Protocol	**1.1**	**2.1**	**2.2**	**3.1**	**3.2**	**4.1**	**4.2**	**4.3**	**4.4**
[Liu:2014] [25]	✓	✓	✓	✓		✓		✓	✓
Alert [26]	✓	✓	✓	✓	✓	✓		✓	✓
BP-MAC [27]	✓	✓	✓	✓		✓	✓	✓	✓
BPS-MAC [28]	✓	✓	✓	✓		✓	✓	✓	✓
CSMA/CA [29]	✓	✓	✓	✓		✓	✓	✓	✓
CSMA/p* [30]	✓	✓	✓	✓	✓	✓	✓	✓	
CSMA-TDMA Hybrid [31]	✓	✓	✓	✓		✓	✓	✓	✓
DSA++ [32]		✓	✓	✓		✓	✓	✓	✓
EY-NPMA [33]	✓	✓	✓	✓	✓	✓	✓	✓	✓
FS-TS-Aloha [23]	✓	✓	✓	✓	✓	✓	✓	✓	✓
FS-TU-Aloha [23]	✓	✓	✓	✓	✓	✓	✓	✓	✓
FU-TS-Aloha [23]	✓	✓	✓	✓	✓	✓	✓	✓	✓
FU-TU-Aloha [23]	✓	✓	✓	✓	✓	✓	✓	✓	✓
ISMA [34]	✓	✓	✓	✓	✓	✓	✓	✓	✓
MASCARA [34]		✓	✓	✓		✓	✓	✓	✓
nanoMAC [35]	✓	✓	✓	✓		✓	✓	✓	✓
non persistent CSMA [36]	✓	✓	✓	✓	✓	✓	✓	✓	✓
persistent CSMA [36]	✓	✓	✓	✓	✓	✓	✓	✓	✓
Pure Aloha [36]	✓	✓	✓	✓	✓	✓	✓	✓	✓
R-ISMA [34]	✓	✓	✓	✓		✓	✓	✓	✓
RMAC [37]	✓	✓	✓	✓		✓	✓	✓	✓
SIFT [38]	✓	✓	✓	✓	✓	✓	✓	✓	✓
Slotted Aloha [36]	✓	✓	✓	✓	✓	✓	✓	✓	✓
TDMA [36]	✓	✓	✓	✓	✓		✓	✓	✓
Others...	See Appendix B								

Table 3.1: Summary of selected MAC protocols.

Protocol	**Category**	**Single channel**
BPMAC	Listen before talk	✓
BPSMAC	Listen before talk	✓
EY-NPMA	Listen before talk	✓
FS-TS-Aloha	Contention	
FS-TU-Aloha	Contention	
FU-TS-Aloha	Contention	
FU-TU-Aloha	Contention	
ISMA	Collision avoidance	✓
non persistent CSMA	Listen before talk	✓
Pure Aloha	Contention	✓
SIFT	Listen before talk	✓
Slotted Aloha	Contention	✓

Table 3.2: Selected protocols and categorization.

that protocol will not be considered. The multi channel protocols from Table 3.2 will be and they are the multi channel counterparts of the Aloha type protocols.

3.3 Multi channel simulation

All FOMs are captured in the simulation. The simulation is done in the case of both 1 ppm or 10 ppm with a variable number of channels and for 10 kHz and 20 kHz bandwidth.

Simulations are performed up to a network load of 400 Erlang. In case of a perfect MAC protocol the bandwidth of 20 kHz gives room for approximately 200 channels, each with a maximum network load of 1 Erlang. Since the ideal MAC behavior is not likely to be achieved, a throughput of at most 100 Erlang can be expected.

In figures 3.1 to 3.6 the results of multi channel simulation for the selected protocols are visible as a function of frequency uncertainty and number of channels. The number of channels that perform best in terms of the score at a PDR of 0.9 are compared between each other. These results are given in Table 3.4.

The comparison of the MAC protocols can be seen in figures 3.7 to 3.11.

Category	FU (ppm)	Protocol	G_0	S	ϵ	score	Position
Contention	0	Slotted Aloha	0.90	0.80	0.39	1.70	1
		Pure Aloha	0.24	0.21	0.56	1.26	2
	1	Slotted Aloha	5.21	4.66	0.43	1.82	1
		Pure Aloha	1.85	1.66	0.53	1.36	2
	10	Slotted Aloha	45.91	41.21	0.52	1.92	1
		Pure Aloha	22.01	19.77	0.56	1.48	2
Listen before talk	0	np CSMA	0.30	0.26	0.64	1.91	1
		SIFT	0.33	0.29	0.57	1.89	2
		BPMAC	0.29	0.25	0.63	1.85	3
		BPSMAC	0.29	0.25	0.62	1.85	4
		EY-NPMA	0.32	0.28	0.56	1.84	5
	1	np CSMA	2.19	1.97	0.63	2.00	1
		BPMAC	2.11	1.89	0.61	1.94	2
		BPSMAC	2.10	1.88	0.61	1.93	3
		SIFT	2.18	1.95	0.54	1.86	4
		EY-NPMA	2.18	1.95	0.54	1.85	5
	10	np CSMA	23.86	21.35	0.68	2.00	1
		BPMAC	22.71	20.35	0.66	1.92	2
		BPSMAC	22.64	20.29	0.65	1.91	3
		SIFT	23.36	20.88	0.59	1.85	4
		EY-NPMA	23.64	21.14	0.58	1.85	5
Collision avoidance	0	ISMA	0.46	0.41	0.51	2.00	1
	1	ISMA	2.76	2.48	0.52	2.00	1
	10	ISMA	24.65	22.04	0.61	2.00	2

Table 3.3: Per category results of single channel simulation.

	Number of channels	6	12	18	24
1 ppm	FS-TU-Aloha	1.45	1.88	**1.99**	1.95
	FS-TS-Aloha	1.56	1.95	1.97	**1.97**
	non persistent CSMA	1.54	1.95	1.95	**1.98**
	Number of channels	2	3	4	10
10 ppm	FS-TU-Aloha	1.82	**1.98**	1.93	1.92
	FS-TS-Aloha	**1.98**	1.92	1.92	1.86
	non persistent CSMA	1.88	**2.00**	1.98	1.94

Table 3.4: The scores calculated per MAC protocol to determine the best number of channels, which is shown in bold font.

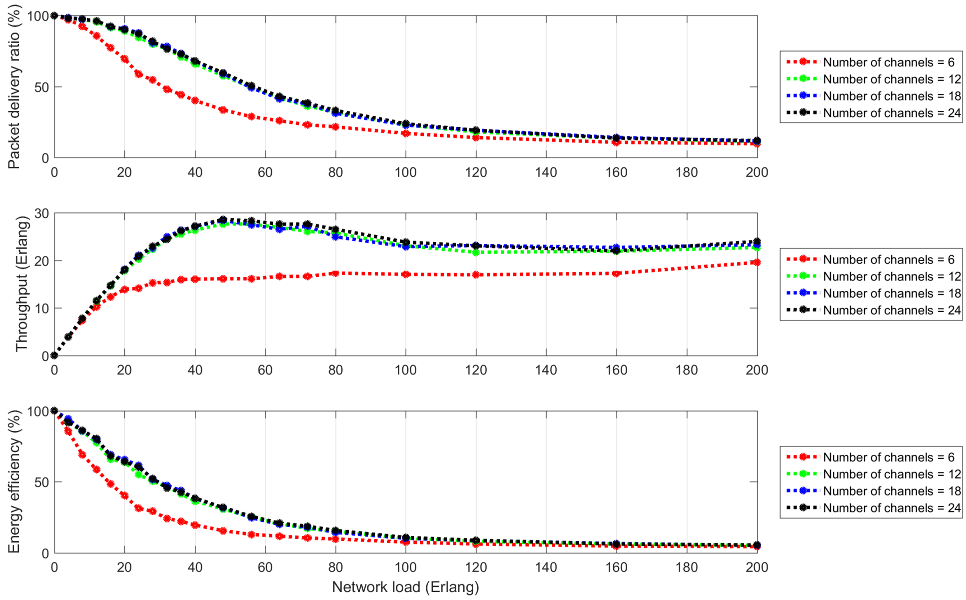

Figure 3.1: FS-TU-Aloha (Pure aloha) multi channel simulation results with 1 ppm frequency uncertainty.

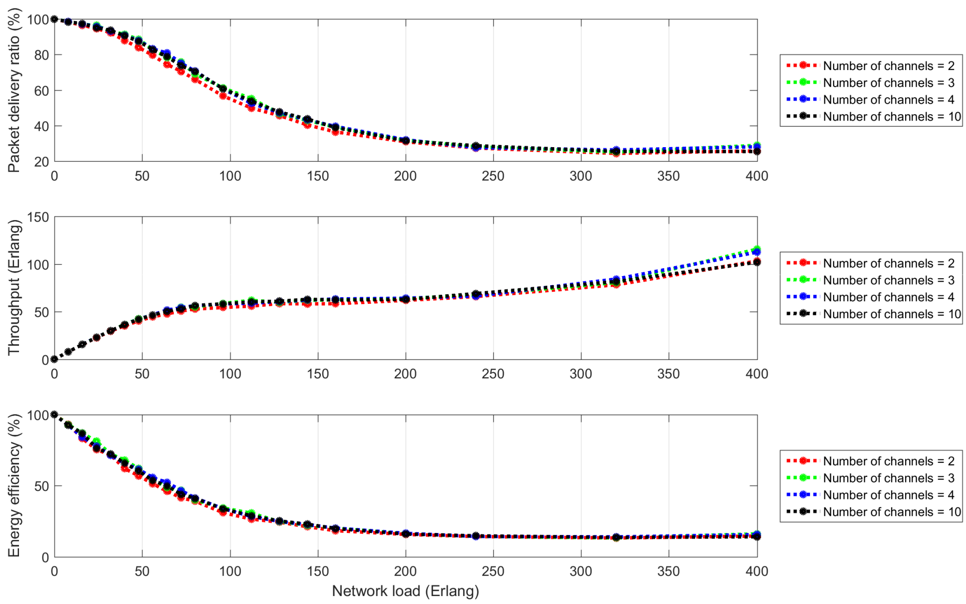

Figure 3.2: FS-TU-Aloha (Pure aloha) multi channel simulation results with 10 ppm frequency uncertainty.

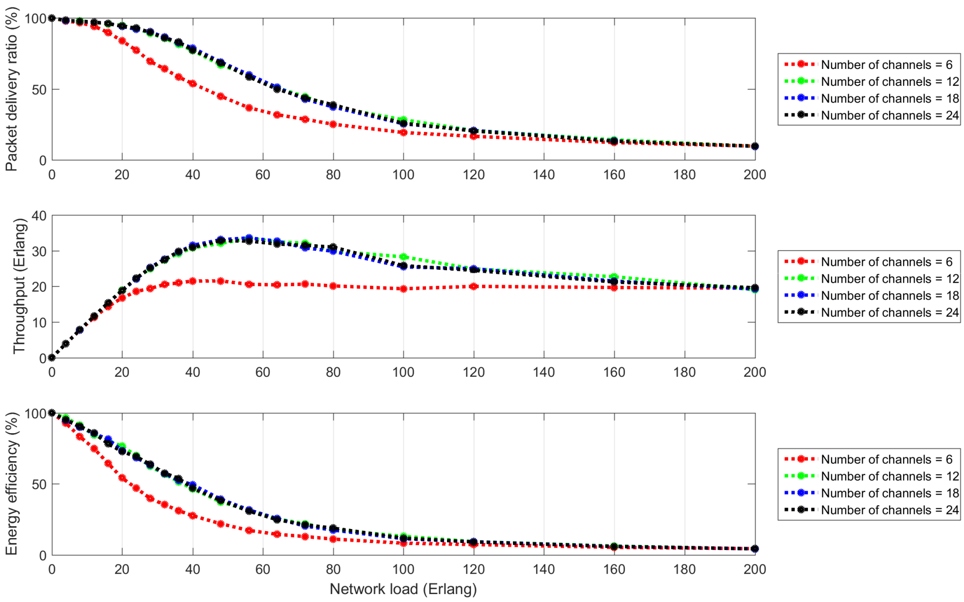

Figure 3.3: FS-TS-Aloha (Slotted Aloha) multi channel simulation results with 1 ppm frequency uncertainty.

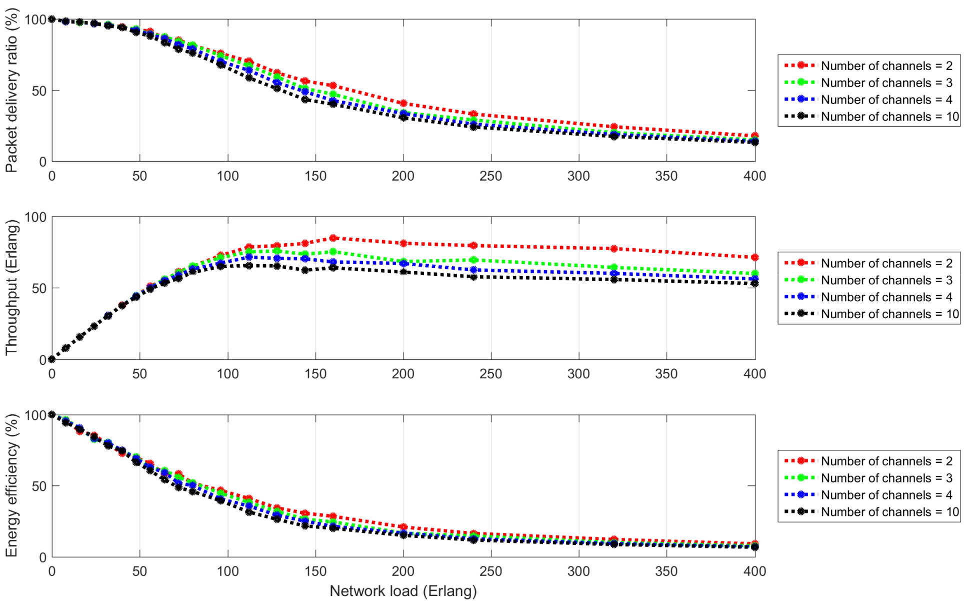

Figure 3.4: FS-TS-Aloha (Slotted Aloha) multi channel simulation results with 10 ppm frequency uncertainty.

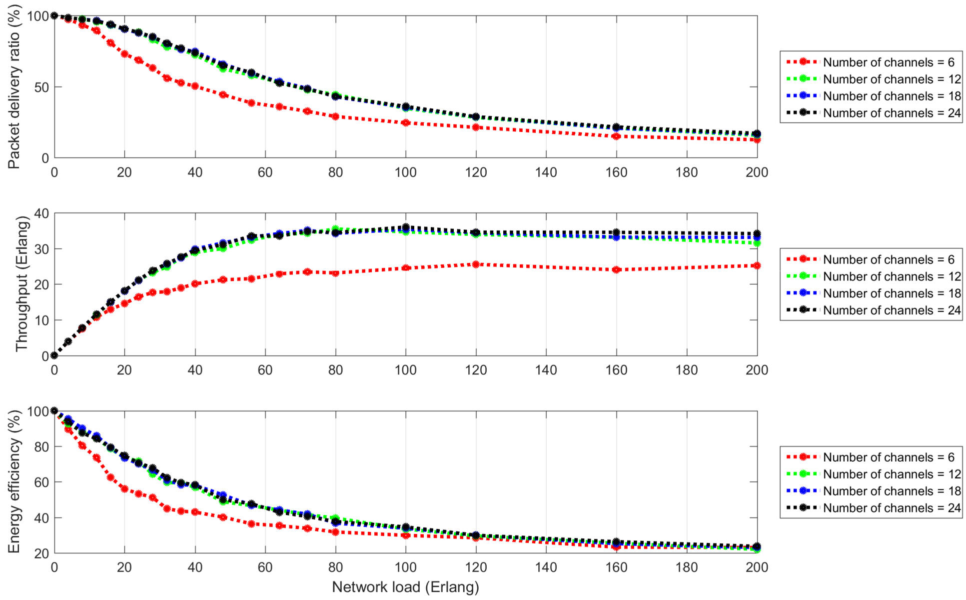

Figure 3.5: Non persistent CSMA multi channel simulation results with 1 ppm frequency uncertainty.

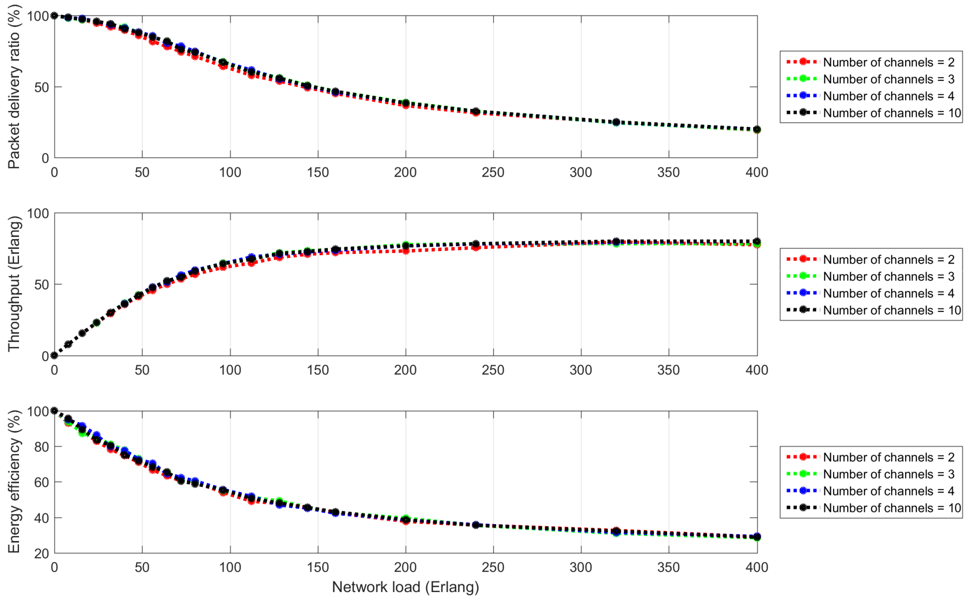

Figure 3.6: Non persistent CSMA multi channel simulation results with 10 ppm frequency uncertainty.

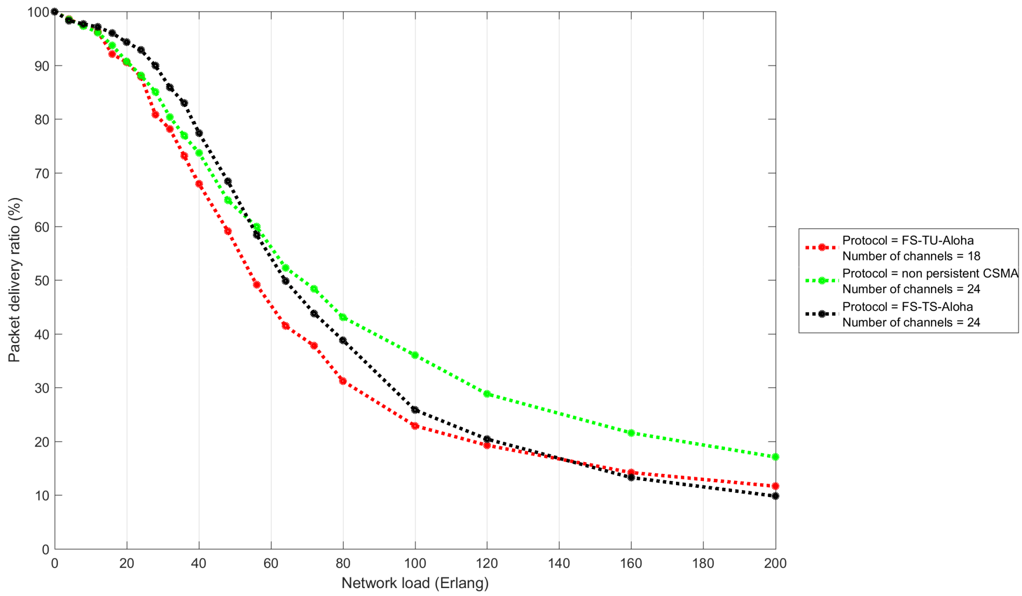

Figure 3.7: Comparison of PDR for multi channel MAC protocols for 1 ppm.

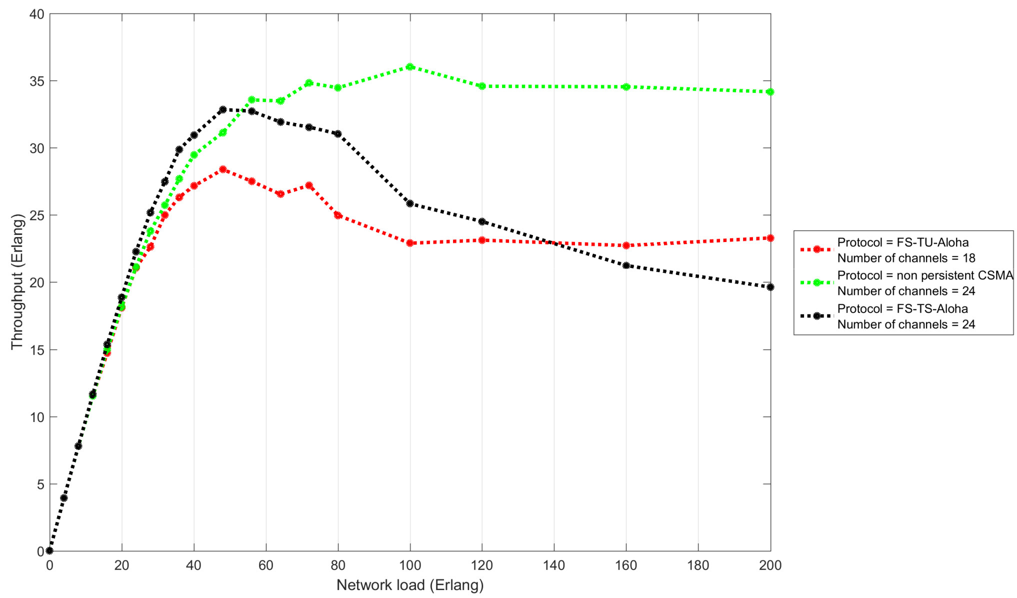

Figure 3.8: Comparison of throughput for multi channel MAC protocols for 1 ppm.

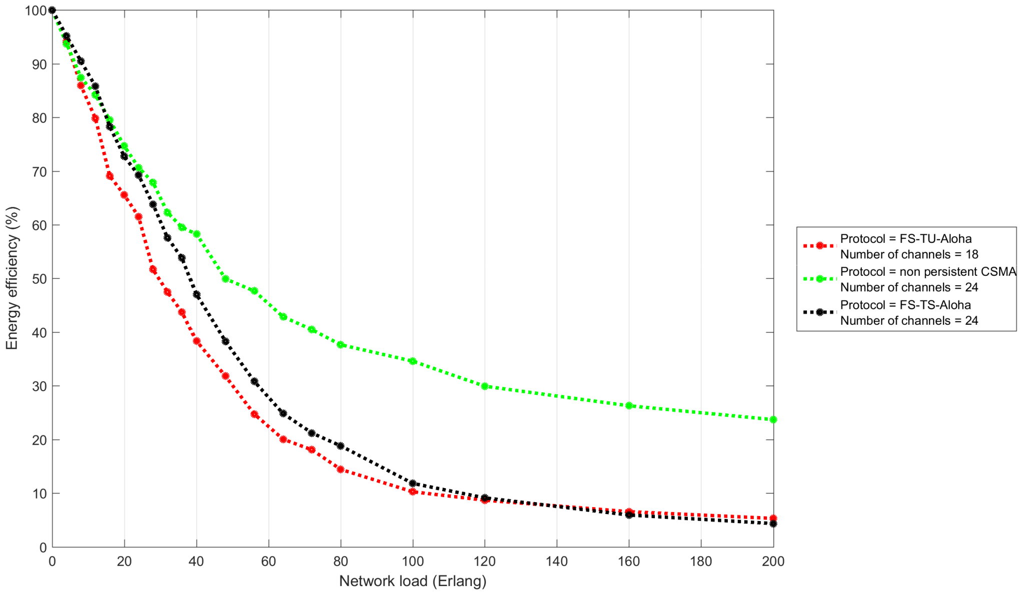

Figure 3.9: Comparison of energy efficiency for multi channel MAC protocols for 1 ppm.

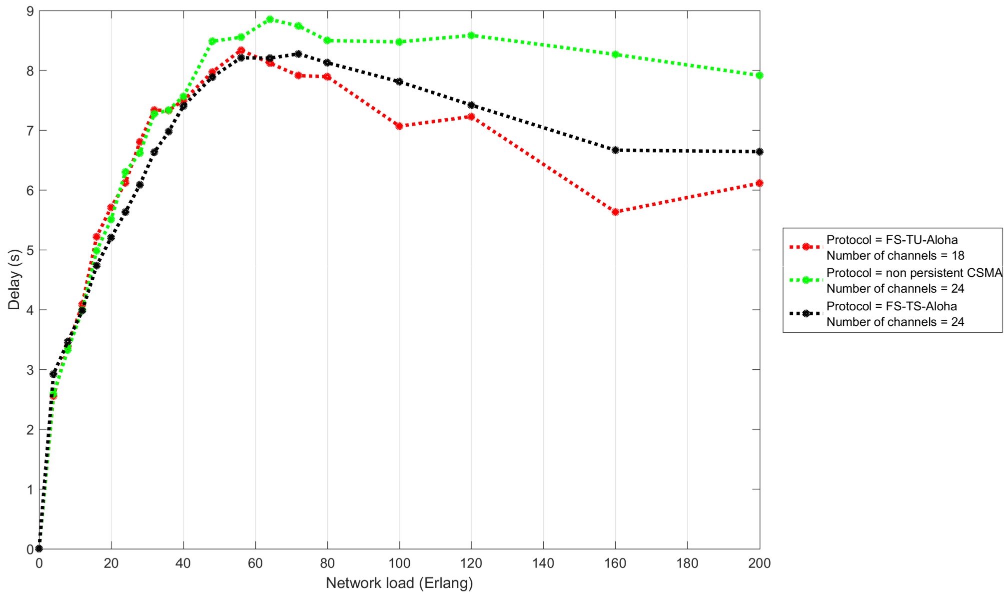

Figure 3.10: Comparison of delay for multi channel MAC protocols for 1 ppm.

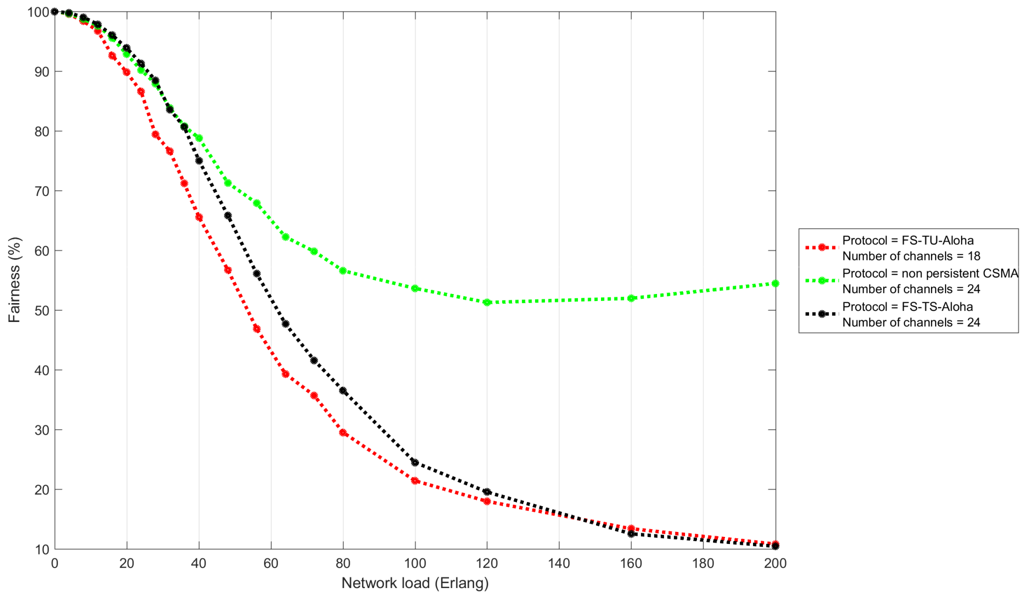

Figure 3.11: Comparison of fairness for multi channel MAC protocols for 1 ppm.

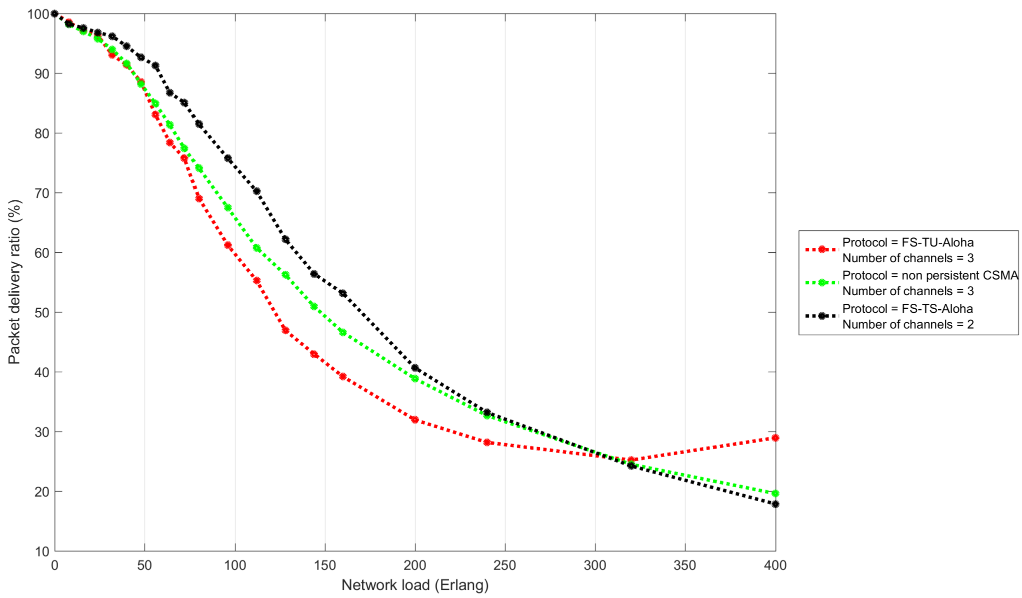

Figure 3.12: Comparison of PDR for multi channel MAC protocols for 10 ppm.

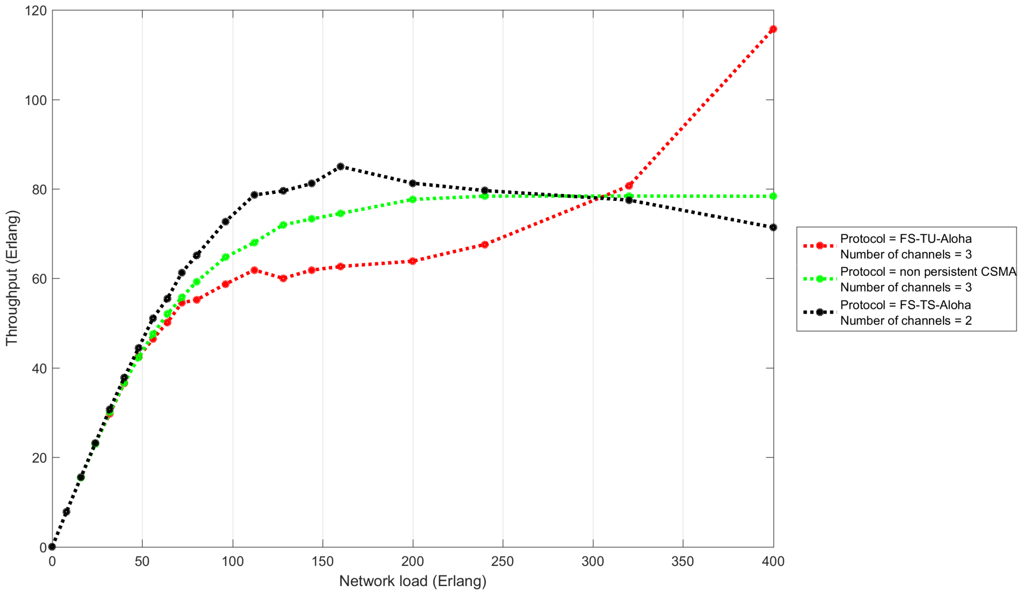

Figure 3.13: Comparison of throughput for multi channel MAC protocols for 10 ppm.

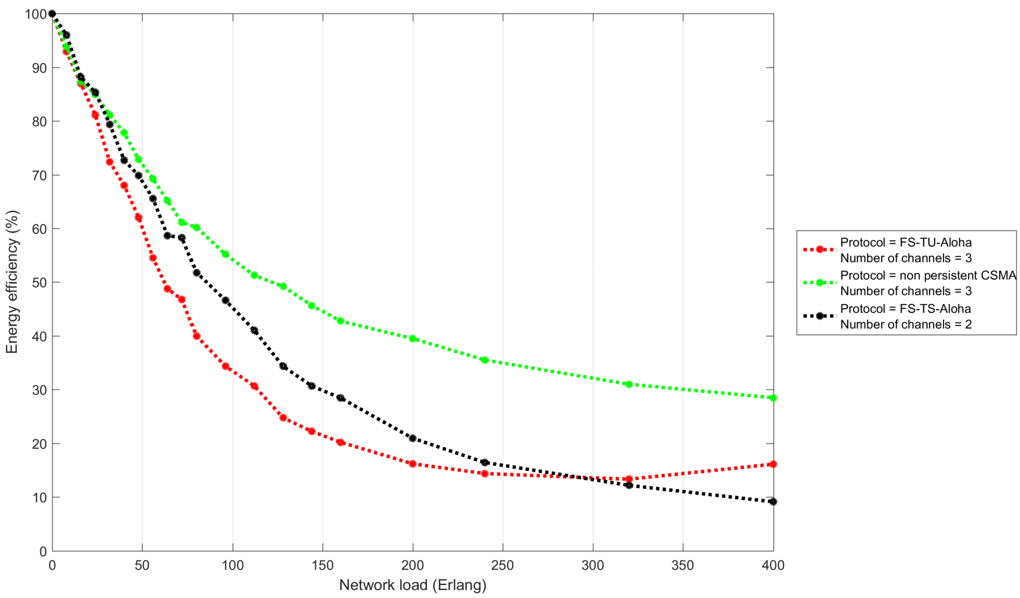

Figure 3.14: Comparison of energy efficiency for multi channel MAC protocols for 10 ppm.

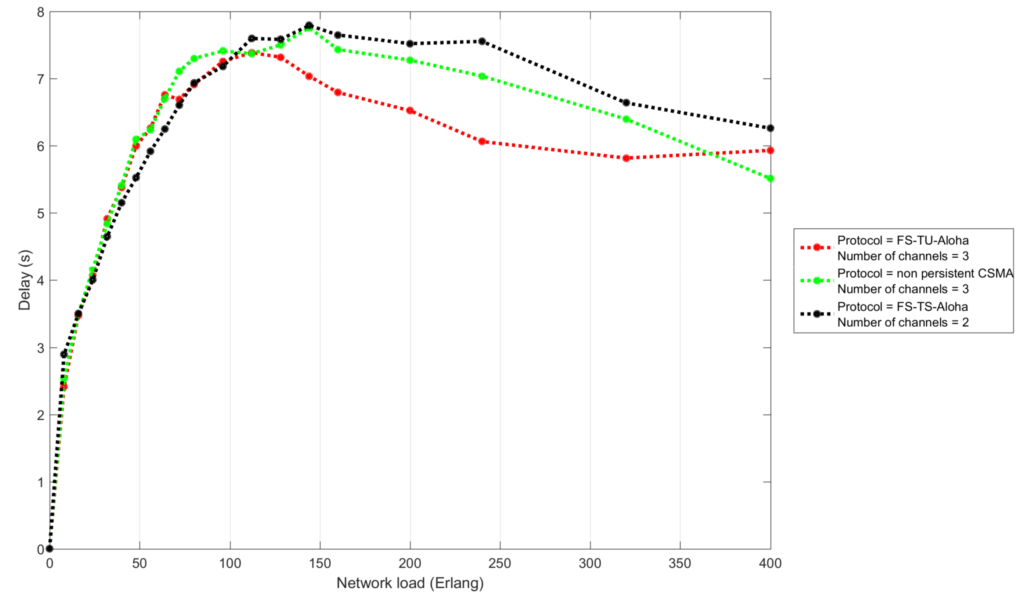

Figure 3.15: Comparison of delay for multi channel MAC protocols for 10 ppm.

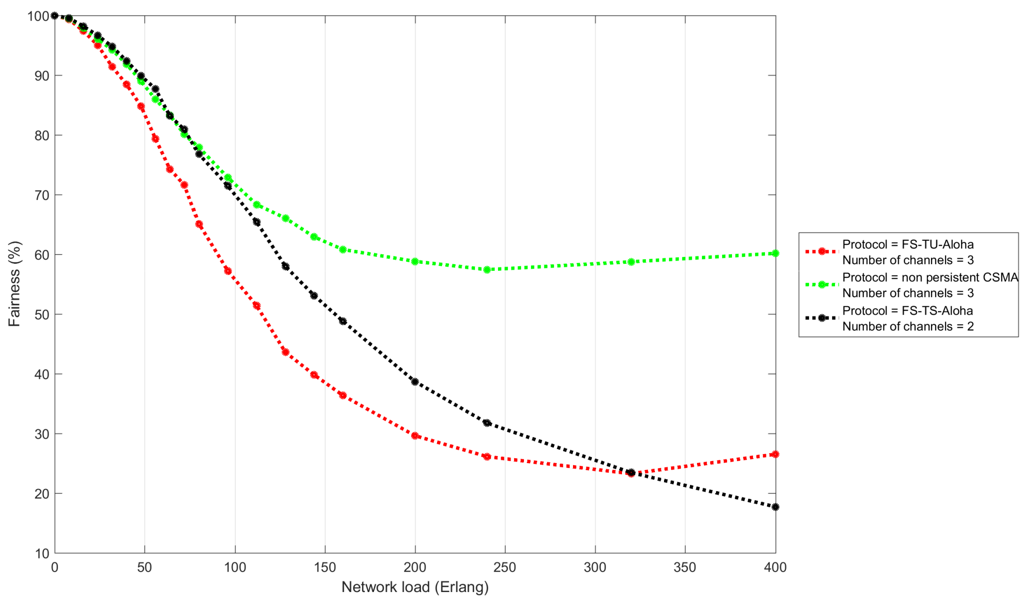

Figure 3.16: Comparison of fairness for multi channel MAC protocols for 10 ppm.

Chapter 4

Discussion

In this chapter the results of simulations are analyzed and discussed. This chapter goes step wise through the methodology applied to discuss the results and to give comments as to why the results are what they are.

4.1 MAC protocol selection

The MAC protocol selection starts with a very large list of which only very few are suitable for further analysis. Many of the dropped protocols have implemented a combination of different layers that built upon a certain basic MAC protocol. While combining MAC protocols with other layers may be beneficial, the protocols that do this cannot be compared fairly to MAC protocols that do not do this. Therefore, only the most basic protocols remain for simulation in this research.

4.2 Single channel simulation

The results of single channel simulation present the effect of frequency uncertainty on MAC protocol performance. Each category has been studied and a comparison has been made between the MAC protocols within that category. Some observations can be made about the results. These are treated per category. Observations of the reference simulations for verification have already been given in Section 2.4.2. The results have been processed into the form of a table to calculate the relative scores. The results of single channel simulation which are referred to in this discussion are in Table 3.3.

4.2.1 Contention

In the contention category there are pure Aloha and slotted Aloha. For each of the simulated frequency uncertainties the slotted Aloha protocol outperforms pure Aloha protocol. This can be explained by the time slotted operation of slotted Aloha. In a time slotted system no partial collisions will appear, such that the channel is better used. With increasing frequency uncertainty more packets can be successfully transmitted at the same time. While this increases throughput of the contention protocols, the bandwidth used for the single channel expands. The effect of frequency uncertainty is roughly the same for both protocols. In other words, since the packets have equal delivery probability the required amount of energy does not change.

4.2.2 Listen before talk

The LBT MAC protocols are SIFT, non-persistent CSMA, BPMAC, BPSMAC and EY-NPMA. SIFT protocol uses a persistent type of CSMA with an optimal distribution for contention resolution. BPMAC, BPSMAC and EY-NPMA use preambles to notify other nodes of an imminent packet as contention resolution. The protocols that use contention resolution are outperformed by the non-persistent CSMA, which doesn't have contention resolution. This can be explained with the used model. Contention resolution does only work when two or more nodes are attempting to access the channel at the same time, given they are not hidden nodes. Furthermore, the contention resolution requires time to give every node a turn. In the Poisson process the probability of two packets being generated at the same time is very low and the rate at which packet are generated does not allow time for the channel to eliminate a congested state of the network. In the Poisson process the probability of time synchronous transmissions does not outweigh the little overhead introduced for contention resolution. The effect of frequency uncertainty is similar as in the contention protocols.

4.2.3 Collision avoidance

In collision avoidance category only the ISMA protocol meets the set criteria. The ISMA protocol uses broadcasted idle packets from the base station to determine whether the channel is free. While this saves energy in the nodes, the scheme places a heavy burden on the downlink channel. Furthermore, when applied to the multi channel scenario the ISMA protocol will require to notify the nodes of the status of each of the channels, every time slot. This scenario is impractical for both reasons of duty cycle restrictions of the downlink and efficient frequency use. Single channel ISMA works alright, even in the presence of frequency uncertainty. This is due to collision avoidance which tries to minimize collisions from hidden nodes, of which there are quite a lot.

4.3 Multi channel simulation

In multi channel simulation the best MAC protocols per category of single channel simulation are compared with each other. The distribution of the center frequency used by a node depends on the number of channels (channel chosen with equal probability and equal spacing) and the frequency uncertainty. The multi channel simulation gives a comparison of performance including the effect of frequency multiplexing.

4.3.1 FS-TU-Aloha

In the case of FS-TU-Aloha, the multi channel counterpart of pure Aloha, the number of channels does make a clear difference for 1 ppm case, as seen in Figure 3.1. For the 10-ppm crystal (Figure 3.2) the FOMs are almost similar. This is due to the shape of the distributions for center frequencies, as can be seen in Figure 2.7. As the 1 ppm case has more resemblance with the uniform distribution of CR-FDMA these results can be trusted when it comes to the number of channels. The scores of FS-TU-Aloha for 18 and 24 channels do not change much just as their frequency distributions.

4.3.2 FS-TS-Aloha

Just as in FS-TU-Aloha, in FS-TS-Aloha the results of figures 3.3 and 3.4 show good behavior for high number of channels in the case of 1 ppm and a low number of channels in the case of 10 ppm. In the 10-ppm case the low number of channel performs slightly better than the high number of channels. This is a remarkable feature. However, since it is not like this for 1 ppm it cannot be concluded that less channels will be better.

4.3.3 Non-persistent CSMA

For non-persistent CSMA, as long as the frequency distribution is like a uniform distribution, the number of channels does not really matter in case of 1 ppm frequency uncertainty, as shown in Figure 3.5. 6 channels clearly performs worse, but the other number of channels do not show large deviations between them. For 10 ppm frequency uncertainty, as shown in Figure 3.6, there is not much difference between any of the number of channels. However, when looking at the scores from Table 3.4 2 channels is performing slightly worse than the other number of channels.

4.3.4 Comparison

The comparison of the FOMs for the best performing MAC protocols in 10 and 20 kHz bandwidth can be found in figures 3.7 to 3.16.

Packet delivery ratio What one can obtain clearly from Figure 3.7 is that FS-TS-Aloha outperforms the other protocols based on PDR. Especially when looking at 90% value, the FS-TS-Aloha performs better than the other protocols. With a much higher network load the CSMA protocol takes over. The same goes approximately for 10 ppm frequency uncertainty, as seen in Figure 3.12.

Throughput For throughput the same arguments apply as in PDR, since the two are highly related. This can be seen in figures 3.8 and 3.13. There is some strange behavior happening at FS-TU-Aloha throughput at very high network load. The throughput goes up again, this can be explained as a side effect of the simulations that may be introduced because of the capture effect and the low number of nodes that contribute to the performance. The region where this effect happens is not of interest to anyone who uses the system as it as less than 30 % packet delivery ratio.

Energy efficiency The energy efficiency can be compared from figures 3.9 and 3.14. The energy efficiency goes down quite fast. The network is therefore best run at a low network load. For both 1 and 10 ppm cases the energy efficiency is best at non-persistent CSMA.

Delay All protocols have comparable average delay, which can be seen in figures 3.10 and 3.15. The least delay occurs at FS-TS-Aloha, because it requires less retransmissions. Since the number of attempts of non-persistent CSMA is limited, the delay is also bounded. This ensures good behavior in terms of the FOMs, but additional delay may be traded off at the gain of PDR. In the region of low network load FS-TS-Aloha has slightly higher delay because of the packets that have to wait before a new time slot starts.

Fairness The fairness of the MAC protocols is quite a smooth curve as shown in figures 3.11 and 3.16. The capture effect will cause unfair behavior, because the nodes nearby the base station are the only ones able to transmit their packets and have them received correctly. Non-persistent CSMA is the only protocol that remains to have some fairness at high network load. The Aloha protocols are unfair and are not equipped with the tools to redistribute the medium access.

Chapter 5

Conclusions and recommendations

Suitable MAC protocols for a UNB communication system have been collected and compared based on their performance in a single channel and multi channel environment. Path loss and frequency uncertainty are physical effects that have been modeled. Retransmissions have been used to upgrade the reliability of the protocol. The results for the situations have been explained in Chapter 4. In this chapter the conclusions are drawn from the results of simulation and in Section 5.2 recommendations are made for follow-up research.

5.1 Conclusions

Based on the simulations presented in the results chapter it can be concluded that path loss is one of the physical effects that has a large influence on MAC protocol performance. It causes hidden nodes and allows for capture effect. Where the capture effect poses an improvement of throughput, the same cannot be said for hidden nodes. Hidden nodes make that CSMA protocols perform even worse than slotted Aloha or FS-TS-Aloha, while in theory its performance should be much better. A quantitative conclusion cannot be drawn on the effect of hidden nodes for CSMA protocols, because only one situation of hidden nodes is researched. Collision avoidance or reservation protocols will not be suitable for UNB communication systems with rare, short packets.

The effect of frequency uncertainty is large on single channel UNB networks, because of the small signal bandwidth compared to the large frequency uncertainty. This enables the ability to have frequency multiplexing on a single channel, such that no errors are caused. However, it does require an intelligent receiver to find and demodulate all the signals. This will be possible in a star topology, where the base station is equipped with unlimited resources.

In a multi channel network the frequency division access technique that shows the best performance is CR-FDMA. While this can be seen from the 1 ppm graphs, the 10 ppm graphs show different behavior. As this is a side effect of the limited bandwidth used for simulation the 1 ppm shows that a uniform distribution makes better use of the spectrum than largely separated channels. The CR-FDMA has as additional benefit that frequency uncertainty does not influence the performance of the node. Only at the edges of the bandwidth the frequency uncertainty can cause the node to transmit outside the intended band. With increasing frequency uncertainty the probability that this happens becomes larger. This can be counteracted by reducing the allowed error probability or the number of channels.

Using a time slotted protocol reduces the probability of collision, because time uncertainty and propagation time are relatively very short compared to the packet transmission time.

For the uplink of nodes in a UNB star topology network the best MAC protocol depends on the physical properties of the channel. Slotted Aloha shows the best performance in the simulation. However, the probability of hidden nodes has influence on the performance of CSMA. The range at which nodes are able to sense influences the number of hidden nodes and thus the performance of CSMA.

5.2 Recommendations

The first recommendation I make is that the simulation setup may be improved, as it has been designed for accuracy of the model instead of speed. This means that the accuracy of the simulation results is limited, because of the number of simulations that could have been performed in the available time. Before more simulations are started, the speed of the simulation process should be improved. If the simulation speed in increased the accuracy of simulations can be increased by the use of Monte Carlo simulation runs.

In the simulations the infinite node assumption is approximated with a high number of nodes. However, this approximation is invalidated at high delay and network load. To prevent this problem and be able to increase network load even further it is necessary to adjust the simulation to create nodes dynamically and with that change the model into a real infinite node situation.

As indicated in Section 2.2.5 the phase noise generated at the node and the fading characteristics have not been included in this research. Further study can be done by including phase noise and fading into the model, as these do affect performance of the system and may lead to a different conclusion.

Because of the choice for a Poisson process a major drawback of the Aloha protocols has not been exposed. The effect of spatially correlated packet may be investigated in further research, because it is likely to occur in WSNs. It can be expected that LBT protocols have better performance in such a system and preamble based protocols may be useful to boost the performance. Whereas in this research the preamble was just a wast of energy, if contention is required due to correlated packet generation it might be just the right thing to do.

CR-FDMA has been shown to have good performance in a situation of relatively high bandwidth, but not for low bandwidth. As the summation of Gaussian distributions does never totally combine into a uniform distribution, the smaller the bandwidth the worse the fit. Which distribution is ideal as a function of signal bandwidth, channel bandwidth and frequency uncertainty may be a topic of further research.

As concluded, the hidden nodes have large influence on the performance of LBT protocols. A feasibility study can be done to determine if the probability of hidden nodes can be minimized (by finding the possible range of the RSSI measurement) to make LBT protocols perform better.

In this research only the most basic MAC protocols have been studied. It may be interesting to create a MAC protocol that combines the best aspects of these protocols. Slotted time, listen before talk and preamble contention resolution may be combined in a way to constitute a MAC protocol that outperforms the ones studied here.

Chapter 6

Acknowledgments

The thesis I have been starting to work on in September 2016 is finally starting to come to an end. In the process I have had ups and downs, but my supervisor Zaher Mahfouz was always there for support, for which I wish to express my gratitude. Many things have changed during the last year. My girlfriend Mariëlle Gaster has always believed in me and was a good motivation, especially since she is with child. Others I would like to thank are Arjan Meijerink and Mark Bentum for giving me the opportunity to write a master's thesis and helping me out when I was distressed.

Bibliography

[1] F. J. Oppermann, C. A. Boano, and K. Römer, *A Decade of Wireless Sensing Applications: Survey and Taxonomy*. Berlin, Heidelberg: Springer Berlin Heidelberg, 2014, pp. 11–50. [Online]. Available: http://dx.doi.org/10.1007/978-3-642-40009-4_2

[2] I. F. Akyildiz, W. Su, Y. Sankarasubramaniam, and E. Cayirci, "A survey on sensor networks," *IEEE Communications Magazine*, vol. 40, no. 8, pp. 102–114, Aug 2002.

[3] S. Drago, F. Sebastiano, L. J. Breems, D. M. W. Leenaerts, K. A. A. Makinwa, and B. Nauta, "Impulse-based scheme for crystal-less ulp radios," *IEEE Transactions on Circuits and Systems I: Regular Papers*, vol. 56, no. 5, pp. 1041–1052, May 2009.

[4] "Radio technology keypoints — sigfox." [Online]. Available: https://www.sigfox.com/en/sigfox-iot-radio-technology

[5] *CC1021 Single Chip Low Power RF Transceiver for Narrowband Systems*, Texas Instruments, 08 2006, rev. SWRS045E.

[6] M.-T. Do, "Ultra narrowband wireless sensor networks modeling and optimization," Ph.D. dissertation, l'Institut National des Sciences Appliques de Lyon, 2015.

[7] L. Kleinrock and F. Tobagi, "Packet switching in radio channels: Part i - carrier sense multiple-access modes and their throughput-delay characteristics," *IEEE Transactions on Communications*, vol. 23, no. 12, pp. 1400–1416, December 1975.

[8] "Slow wireless." [Online]. Available: https://www.utwente.nl/ewi/te/projects/SRR/slow_wireless/

[9] D. Torrieri, *Principles of spread-spectrum communication systems*. Springer, 2005.

[10] N. Abramson, "The throughput of packet broadcasting channels," *IEEE Transactions on Communications*, vol. 25, no. 1, pp. 117–128, Jan 1977.

[11] S. Haykin, *Introduction to Analog and Digital Communications*. John Wiley & Sons, Inc., 2007.

[12] M. Anteur, V. Deslandes, N. Thomas, and A. L. Beylot, "Ultra narrow band technique for low power wide area communications," in *2015 IEEE Global Communications Conference (GLOBECOM)*, Dec 2015, pp. 1–6.

[13] P. Liu, Y. Bar-Ness, and J. Zhu, "Effects of phase noise at both transmitter and receiver on the performance of ofdm systems," in *2006 40th Annual Conference on Information Sciences and Systems*, March 2006, pp. 312–316.

[14] S. Hussain and S. K. Barton, "The performance of coherent bpsk in the presence of oscillator phase noise for ka-band pico-terminal inbound links," *Wireless Personal Communications*, vol. 1, no. 2, pp. 111–115, Jun 1994. [Online]. Available: http://dx.doi.org/10.1007/BF01098688

[15] A. Goldsmith, *Wireless communications*. Stanford University, 2004.

[16] M. F. Khan, E. A. Felemban, S. Qaisar, and S. Ali, "Performance analysis on packet delivery ratio and end-to-end delay of different network topologies in wireless sensor networks (wsns)," in *2013 IEEE 9th International Conference on Mobile Ad-hoc and Sensor Networks*, Dec 2013, pp. 324–329.

[17] R. Jain, D.-M. Chiu, and W. R. Hawe, *A quantitative measure of fairness and discrimination for resource allocation in shared computer system*. Eastern Research Laboratory, Digital Equipment Corporation Hudson, MA, 1984, vol. 38.

[18] N. Xie and S. Weber, "On the aloha throughput-fairness tradeoff," *IEEE Transactions on Information Theory*, vol. PP, no. 99, pp. 1–1, 2017.

[19] H. Karl and A. Willig, *Protocols and Architectures for Wireless Sensor Networks*. John Wiley & Sons Ltd., 2005.

[20] *Single-Chip SIGFOX RF Transceiver*, Atmel Corporation, 09 2016, rev. 9409C-09/16.

[21] A. Willig, "Recent and emerging topics in wireless industrial communications: A selection," *IEEE Transactions on Industrial Informatics*, vol. 4, no. 2, pp. 102–124, May 2008.

[22] O. Ltd., "Omnet++." [Online]. Available: https://omnetpp.org/

[23] C. Goursaud and Y. Mo, “Random unslotted time-frequency aloha: Theory and application to iot unb networks,” in *2016 23rd International Conference on Telecommunications (ICT)*, May 2016, pp. 1–5.

[24] S. Drago, F. Sebastiano, L. J. Breems, D. M. W. Leenaerts, K. A. A. Makinwa, and B. Nauta, “Impulse-based scheme for crystal-less ulp radios,” *IEEE Transactions on Circuits and Systems I: Regular Papers*, vol. 56, no. 5, pp. 1041–1052, May 2009.

[25] Y. Liu, C. Yuen, X. Cao, N. U. Hassan, and J. Chen, “Design of a scalable hybrid mac protocol for heterogeneous m2m networks,” *IEEE Internet of Things Journal*, vol. 1, no. 1, pp. 99–111, Feb 2014.

[26] V. Namboodiri and A. Keshavarzian, “Alert: An adaptive low-latency event-driven mac protocol for wireless sensor networks,” in *2008 International Conference on Information Processing in Sensor Networks (ipsn 2008)*, April 2008, pp. 159–170.

[27] A. Klein, J. Klaue, and J. Schalk, “Bp-mac: a high reliable backoff preamble mac protocol for wireless sensor networks,” *Electronic Journal of Structural Engineering (EJSE): Special Issue of Sensor Networks for Building Monitoring: From Theory to Real Application*, pp. 35–45, 2009.

[28] A. Klein, *BPS-MAC: Backoff Preamble Based MAC Protocol with Sequential Contention Resolution*. Berlin, Heidelberg: Springer Berlin Heidelberg, 2011, pp. 39–50. [Online]. Available: http://dx.doi.org/10.1007/978-3-642-23795-9_4

[29] E. Ziouva and T. Antonakopoulos, “Csma/ca performance under high traffic conditions: throughput and delay analysis,” *Computer communications*, vol. 25, no. 3, pp. 313–321, 2002.

[30] Y. C. Tay, K. Jamieson, and H. Balakrishnan, “Collision-minimizing csma and its applications to wireless sensor networks,” *IEEE Journal on Selected Areas in Communications*, vol. 22, no. 6, pp. 1048–1057, Aug 2004.

[31] Y. Liu, C. Yuen, J. Chen, and X. Cao, “A scalable hybrid mac protocol for massive m2m networks,” in *2013 IEEE Wireless Communications and Networking Conference (WCNC)*, April 2013, pp. 250–255.

[32] C. Deqin, “Study on mac dsa++ protocols for wireless networks.”

[33] K. Fu, Y. Guo, and S. Barton, “Performance of the ey-npma protocol,” *Wireless Personal Communications*, vol. 4, no. 1, pp. 41–50, 1997. [Online]. Available: http://dx.doi.org/10.1023/A:1008842203886

[34] A. C. V. Gummalla and J. O. Limb, "Wireless medium access control protocols," *IEEE Communications Surveys Tutorials*, vol. 3, no. 2, pp. 2–15, Second 2000.

[35] J. Haapola, "Nanomac: A distributed mac protocol for wireless ad hoc sensor networks," in *XXXVII Convention on Radio Science & IV Finnish Wireless Communication Workshop*, 2003.

[36] I. Stojmenovic, *Handbook of sensor networks: algorithms and architectures*. John Wiley & Sons, 2005, vol. 49.

[37] S. Datta, "Rmac: a randomized adaptive medium access control algorithm for sensor networks," in *proceedings of the Second Workshop on Sensor and Actor Networks and Protocols (SANPA'04)*. Citeseer, 2004.

[38] K. Jamieson, H. Balakrishnan, and Y. Tay, "Sift: A mac protocol for event-driven wireless sensor networks," in *European Workshop on Wireless Sensor Networks*. Springer, 2006, pp. 260–275.

Appendix A

Derivation of physical model parameters

As a start the block diagram of the communication system is taken, as presented in Figure A.1. This means the physical model, which represents the relation between output and input before sampling. The channel is expected to be ideal, meaning no delay, path loss or frequency selectivity occurs and the channel can be replaced with a convolution of a Dirac delta function. Furthermore, the double frequency terms can be neglected.

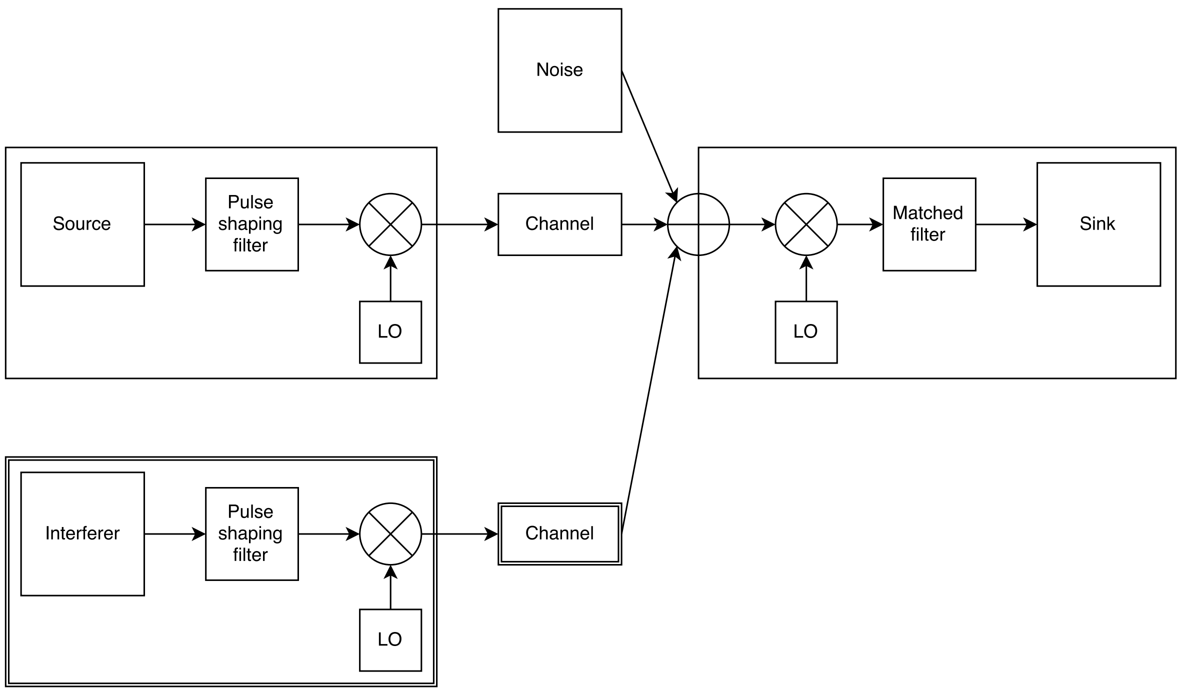

Figure A.1: Block diagram of physical layer model

The signals from the source and the interferers can be described with a pulse train, as shown in Equation A.1. The values of x_n can be either x_0 or $-x_0$, where

x_0 is a constant magnitude of any bit in the stream. The pulses can occur at any time, ϕ_x makes sure of this. We assume the receiver will be able to compensate for static time and phase offset or drift. This means the synchronization of the receiver is assumed to be perfect. In real life the receiver may not be able to lock on to the signal such that the signal is lost.

$$x(t) = \sum_{n \in \mathbb{Z}} x_n \delta(t - nT - \phi_x) \tag{A.1}$$

As can be noted from the block diagram, there may be a multiple number of interferers. In the AWGN model, in combination with the SINR model, the different sources of interference are considered to be independent. Therefore the contribution of the noise can be treated separately and the result of the noise from interference, or rejection coëfficient β, can be multiplied with the number of interfering nodes to retrieve the aggregate interference level.

$$\begin{aligned} z(t) = & \frac{A_x A_z}{2} \sum_{n \in \mathbb{Z}} x_n \int_{-\infty}^{\infty} \cos((\omega_x - \omega_z)x_3 + \theta_x - \theta_z) p_t(x_3 - nT - \phi_x) p_r(t - x_3)\, dx_3 \\ & + \frac{A_y A_z}{2} \sum_{k \in \mathbb{Z}} y_k \int_{-\infty}^{\infty} \cos((\omega_y - \omega_z)x_3 + \theta_y - \theta_z) p_t(x_3 - kT - \phi_y) p_r(t - x_3)\, dx_3 \\ & + A_z \int_{-\infty}^{\infty} N(x_3) \cos(\omega_z x_3 + \theta_z) p_r(t - x_3)\, dx_3 \end{aligned} \tag{A.2}$$

Now if we assume the simplest case of perfect synchronization where $\omega_x = \omega_z$ and $\theta_x = \theta_z$ this simplifies even further.

$$\begin{aligned} z(t) = & \frac{A_x A_z}{2} \sum_{n \in \mathbb{Z}} x_n \int_{-\infty}^{\infty} p_t(x_3 - nT - \phi_x) p_r(t - x_3)\, dx_3 \\ & + \frac{A_y A_z}{2} \sum_{k \in \mathbb{Z}} y_k \int_{-\infty}^{\infty} \cos((\omega_y - \omega_z)x_3 + \theta_y - \theta_z) p_t(x_3 - kT - \phi_y) p_r(t - x_3)\, dx_3 \\ & + A_z \int_{-\infty}^{\infty} N(x_3) \cos(\omega_z x_3 + \theta_z) p_r(t - x_3)\, dx_3 \end{aligned} \tag{A.3}$$

We let ϕ_y, θ_y, θ_x, x_n and y_k be stochastic and independent variables with probability density functions f_{ϕ_y}, f_{θ_x}, f_{x_n} and f_{y_k} respectively. This can be considered a valid approach, since phases are created locally and do not depend on phases of other nodes. Furthermore, discrete bits can be considered independent on previous or following bits. Whiteness bits are generally application specific and a rule cannot be extracted, thus the independent bits is the simplest assumption and not generally true. Some communication systems use scrambling to make the data behavior more white, which is a technique that can be used when trouble is encountered.

We are interested in the output value as a response to a known input bit, therefore the probability density function of $z(t)$ given the first bit being either x_0 or $-x_0$ can be used to find the probability of error for a certain bit. Other parameters of interest are the frequency difference between the source and the interferer $\delta_\omega = \omega_y - \omega_z$, the noise from other sources N_0 and the timing difference between the actual sample and the output sample $\delta_\phi = \phi_x - \phi_z$.

Due to a large amount of noise sources we can assume the central limit theorem leads to a probability density function which is approximated with a Gaussian distribution with equal stochastic characteristics. To construct the Gaussian distribution the required characteristics are the mean $E[z(t)]$ and auto correlation $E[z(t)z(t+\tau)]$. These can be derived from the system model and variables.

$$
\begin{aligned}
E[z(t)] = {} & \frac{A_x A_z}{2} \sum_{n \in \mathbb{Z}_{\neq 0}} E[x_n] \int_{-\infty}^{\infty} p_t(x_3 - nT - \phi_x) p_r(t - x_3)\, dx_3 \\
& + \frac{A_y A_z}{2} \sum_{k \in \mathbb{Z}} E[y_k] \int_{-\infty}^{\infty} E[\cos(\delta_\omega x_3 + \theta_y - \theta_z)] E[p_t(x_3 - kT - \phi_y)] p_r(t - x_3)\, dx_3 \\
& + A_z \int_{-\infty}^{\infty} E[N(x_3)] E[\cos(\omega_z x_3 + \theta_z)] p_r(t - x_3)\, dx_3 \\
& + \frac{A_x A_z x_0}{2} \int_{-\infty}^{\infty} p_t(x_3 - \phi_x) p_r(t - x_3)\, dx_3
\end{aligned}
\tag{A.4}
$$

Now x_n is either equal to x_0 or $-x_0$ with equal probability, resulting in a mean value of zero and a variance of x_0^2. Along with this the noise has zero mean and some variance depending on N_0, this results in Equation A.5. Then the integral can be converted into a convolution, denoted with $*$.

$$
\begin{aligned}
E[z(t)] &= \frac{A_x A_z x_0}{2} \int_{-\infty}^{\infty} p_t(x_3 - \phi_x) p_r(t - x_3)\, dx_3 \\
&= \frac{A_x A_z x_0}{2} \cdot \Big\{ p_t(\tau_1) * p_r(\tau_1) \Big\}_{\tau_1 = t - \phi_x}
\end{aligned}
\tag{A.5}
$$

The auto correlation of the signal can also be calculated. It is important to note here, that due to the independence of variables the cross terms (terms coming from different sources) will not result in any correlation. This is because the expected value of the white Gaussian noise is zero, i.e. $E[N(t)] = 0$ and $E[x_n y_k] =$

$E[x_n]E[y_k] = 0$.

$$
\begin{aligned}
z(t)z(t+\tau) = &\left\{ \frac{A_x A_z}{2} \sum_{n\in\mathbb{Z}} x_n \int_{-\infty}^{\infty} p_t(x_3 - nT - \phi_x) p_r(t - x_3)\, dx_3 \right. \\
&+ \frac{A_y A_z}{2} \sum_{k\in\mathbb{Z}} y_k \int_{-\infty}^{\infty} \cos((\omega_y - \omega_z)x_3 + \theta_y - \theta_z) p_t(x_3 - kT - \phi_y) p_r(t - x_3)\, dx_3 \\
&\left. + A_z \int_{-\infty}^{\infty} N(x_3) \cos(\omega_z x_3 + \theta_z) p_r(t - x_3)\, dx_3 \right\} \\
&\times \\
&\left\{ \frac{A_x A_z}{2} \sum_{l\in\mathbb{Z}} x_l \int_{-\infty}^{\infty} p_t(x_4 - lT - \phi_x) p_r(t + \tau - x_4)\, dx_4 \right. \\
&+ \frac{A_y A_z}{2} \sum_{m\in\mathbb{Z}} y_m \int_{-\infty}^{\infty} \cos(\delta_\omega x_4 + \theta_y - \theta_z) p_t(x_4 - mT - \phi_y) p_r(t + \tau - x_4)\, dx_4 \\
&\left. + A_z \int_{-\infty}^{\infty} N(x_4) \cos(\omega_z x_4 + \theta_z) p_r(t + \tau - x_4)\, dx_4 \right\}
\end{aligned}
\tag{A.6}
$$

As said the cross terms of Equation A.6 will disappear when the expected value is taken.

$$
\begin{aligned}
E[z(t)z(t+\tau)] = &\left(\frac{A_x A_z}{2}\right)^2 \sum_{n\in\mathbb{Z}} \sum_{l\in\mathbb{Z}} E[x_n x_l] \int_{-\infty}^{\infty} \int_{-\infty}^{\infty} \\
&p_t(x_3 - nT - \phi_x) p_t(x_4 - lT - \phi_x) p_r(t - x_3) p_r(t + \tau - x_4)\, dx_3\, dx_4 \\
&+ \left(\frac{A_y A_z}{2}\right)^2 \sum_{k\in\mathbb{Z}} \sum_{m\in\mathbb{Z}} E[y_k y_m] \int_{-\infty}^{\infty} \int_{-\infty}^{\infty} E\Big[\cos(\delta_\omega x_3 + \theta_y - \theta_z) \cos(\delta_\omega x_4 + \theta_y - \theta_z) \Big] \\
&E\Big[p_t(x_3 - kT - \phi_y) p_t(x_4 - mT - \phi_y) \Big] p_r(t - x_3) p_r(t + \tau - x_4)\, dx_3\, dx_4 \\
&+ A_z^2 \int_{-\infty}^{\infty} \int_{-\infty}^{\infty} E[N(x_3)N(x_4)] E\Big[\cos(\omega_z x_3 + \theta_z) \cos(\omega_z x_4 + \theta_z) \Big] \\
&p_r(t - x_3) p_r(t + \tau - x_4)\, dx_3\, dx_4
\end{aligned}
\tag{A.7}
$$

Now some of these expected values can be simplified any further as shown in Equations A.8, A.9, A.10, A.11, A.12 and A.13, to rewrite Equation A.7 into Equation A.14.

$$
E[x_n x_l] = \delta_k(n - l) x_0^2 \tag{A.8}
$$

Equations A.8 and A.9 are the same, except for the case $n = 0$, which is deterministic. Because of the BPSK communication the mean of a single sample is zero, however when $n = l$ the value is always the same, i.e. $x_n = x_l$. δ_k in this situation is the Kronecker delta function.

$$E[y_k y_m] = \delta_k(k - m)y_0^2 \tag{A.9}$$

In Equation A.10 the expected value of a regular cosine is given. Because the phase offset of the LO is uniformly distributed the cosine will end up as being zero. The quadrature signal is not demodulated for BPSK and will be filtered out, we end up with half the signal strength.

$$\begin{aligned} E\Big[\cos(\delta_\omega x_3 + \theta_y - \theta_z)\cos(\delta_\omega x_4 + \theta_y - \theta_z)\Big] \\ = \frac{1}{2}\cos(\delta_\omega(x_3 - x_4)) + \frac{1}{2}E[\cos(\delta_\omega(x_3 + x_4) + 2\theta_y - 2\theta_z)] \\ = \frac{1}{2}\cos(\delta_\omega(x_3 - x_4)) \end{aligned} \tag{A.10}$$

The exact timing of an interfering signal is not known in advance, therefore it can be between $-T/2$ and $T/2$ with a uniform distribution. The expected value changes into an integral with the distribution in between, as shown in Equation A.11.

$$\begin{aligned} E\Big[p_t(x_3 - kT - \phi_y)p_t(x_4 - mT - \phi_y)\Big] \\ = \frac{1}{T}\int_{-T/2}^{T/2} p_t(x_3 - kT - \phi_y)p_t(x_4 - mT - \phi_y)\, d\phi_y \end{aligned} \tag{A.11}$$

The noise at each time instant is different and independent, this is a property of white Gaussian noise. The power density of the noise is a given constant as given in Equation A.12.

$$E[N(x_3)N(x_4)] = \frac{N_0}{2}\delta(x_3 - x_4) \tag{A.12}$$

Just like in Equation A.10 the cosine term disappears in Equation A.13. This results in the power being divided, this is due to the quadrature power which does not influence the decision of the receiver.

$$\begin{aligned} E\Big[\cos(\omega_z x_3 + \theta_z)\cos(\omega_z x_4 + \theta_z)\Big] \\ = \frac{1}{2}\cos(\omega_z(x_3 - x_4)) + \frac{1}{2}E[\cos(\omega_z(x_3 + x_4) + 2\theta_z)] \\ = \frac{1}{2}\cos(\omega_z(x_3 - x_4)) \end{aligned} \tag{A.13}$$

All mean values can be filled into Equation A.7 and will result in Equation A.14.

$$\begin{aligned}
E[z(t)z(t+\tau)] = &\left(\frac{A_x A_z x_0}{2}\right)^2 \sum_{n\in\mathbb{Z}} \int_{-\infty}^{\infty}\int_{-\infty}^{\infty} \\
&p_t(x_3 - nT - \phi_x)p_t(x_4 - nT - \phi_x)p_r(t - x_3)p_r(t+\tau-x_4)\,dx_3\,dx_4 \\
&+ \left(\frac{A_y A_z y_0}{2}\right)^2 \frac{1}{2T}\int_{-\infty}^{\infty}\int_{-\infty}^{\infty}\sum_{k\in\mathbb{Z}}\int_{-T/2}^{T/2} \cos(\delta_\omega(x_3 - x_4)) \\
&p_t(x_3 - kT - \phi_y)p_t(x_4 - kT - \phi_y)p_r(t - x_3)p_r(t+\tau-x_4)\,d\phi_y\,dx_3\,dx_4 \\
&+ A_z^2\frac{N_0}{4}\int_{-\infty}^{\infty}\int_{-\infty}^{\infty}\delta(x_3 - x_4)\cos(\omega_z(x_3 - x_4)) \\
&p_r(t - x_3)p_r(t+\tau-x_4)\,dx_3\,dx_4
\end{aligned} \tag{A.14}$$

Now we use a change of variables $x_5 = kT + \phi_y$, which means the integral can be converted into an infinite integral, making it independent of absolute time. Also the delta function can be simplified. And the integrals can be converted into convolutions, as shown in Equation A.15.

$$\begin{aligned}
E[z(t)z(t+\tau)] = &\left(\frac{A_x A_z x_0}{2}\right)^2 \sum_{n\in\mathbb{Z}} \int_{-\infty}^{\infty}\int_{-\infty}^{\infty} \\
&p_t(x_3 - nT - \phi_x)p_t(x_4 - nT - \phi_x)p_r(t - x_3)p_r(t+\tau-x_4)\,dx_3\,dx_4 \\
&+ \left(\frac{A_y A_z y_0}{2}\right)^2 \frac{1}{2T}\int_{-\infty}^{\infty}\int_{-\infty}^{\infty}\int_{-\infty}^{\infty} \cos(\delta_\omega(x_3 - x_4)) \\
&p_t(x_3 - x_5)p_t(x_4 - x_5)p_r(t - x_3)p_r(t+\tau-x_4)\,dx_3\,dx_4\,dx_5 \\
&+ A_z^2\frac{N_0}{4}\int_{-\infty}^{\infty} p_r(t - x_3)p_r(t+\tau-x_3)\,dx_3 \\
&= \frac{A_x^2 A_z^2 x_0^2}{4}\sum_{n\in\mathbb{Z}}\Big\{p_t(\tau_1) * p_r(\tau_1)\Big\}\cdot\Big\{p_t(\tau_2) * p_r(\tau_2)\Big\}\Bigg|_{\substack{\tau_1 = t - nT - \phi_x \\ \tau_2 = t+\tau-nT-\phi_x}} \\
&+ \frac{A_y^2 A_z^2 y_0^2}{8T}\cdot\Big\{(p_t(-\tau) * p_t(\tau))\cdot\cos(\delta_\omega\tau)\Big\} * p_r(-\tau) * p_r(\tau) \\
&+ \frac{A_z^2 N_0}{4}\cdot\Big\{p_r(-\tau) * p_r(\tau)\Big\}
\end{aligned} \tag{A.15}$$

Because of the dependence on the sampling instant the resulting variables are dependent on time. However if we assume a perfect sampling instant the result will be independent of time and the error is minimized. At the instant of $t = \phi_x$, the figures result in the mean and variance shown in Equations A.16 and A.17.

$$\mu = \frac{A_x A_z x_0}{2} \cdot \Big\{ p_t(\tau) * p_r(\tau) \Big\}_{\tau=0} \tag{A.16}$$

$$\begin{aligned} \sigma^2 = & \frac{A_x^2 A_z^2 x_0^2}{4} \sum_{n \in \mathbb{Z}_{\neq 0}} \Big\{ p_t(\tau) * p_r(\tau) \Big\}^2_{\tau=nT} \\ & + \frac{A_y^2 A_z^2 y_0^2}{8T} \cdot \Big\{ (p_t(-\tau) * p_t(\tau)) \cdot \cos(\delta_\omega \tau) \Big\} * p_r(-\tau) * p_r(\tau) \Bigg|_{\tau=0} \\ & + \frac{A_z^2 N_0}{4} \cdot \Big\{ p_r(-\tau) * p_r(\tau) \Big\}_{\tau=0} \end{aligned} \tag{A.17}$$

From these equations can be seen that there are three terms in the variance and a single term in the mean. The three terms correspond to noise from the source, noise from other nodes and background noise, the mean term corresponds to the source. As we assumed the receiver power to be Gaussian distributed. The mean and variance of the received signal can be projected onto the Gaussian probability density function shown in Equation A.18. There are two areas which correspond to a bit error, when a 1 has been transmitted and the decision boundary (zero for BPSK) has been crossed, and vice versa.

$$f_x(x) = \frac{1}{\sqrt{2\pi\sigma^2}} \exp \frac{-(x-\mu)^2}{2\sigma^2} \tag{A.18}$$

The probability of error for each bit can be calculated and is given in Equation A.20. α, β and γ are the signal to noise ratios of the resulting signal and can be further specified as in A.21, to simplify the γ component the signal power is required. This can be calculated and might be set to certain value. The transmitted power is the amount of power after the modulator of the transmitter and is given in Equation A.19.

$$\begin{aligned} E[x(t) \cdot x(t+\tau)] &= \frac{A_x^2 x_0^2}{2T} \cos(\omega_x \tau) \{ p_t(-\tau) * p_t(\tau) \} \\ P_x = E[x(t)x(t)] &= \frac{A_x^2 x_0^2}{2T} \Big\{ p_t(-\tau) * p_t(\tau) \Big\}_{\tau=0} \end{aligned} \tag{A.19}$$

The power can be inserted into Equation A.21 to get a single set of variables.

$$\begin{aligned} P(error) &= \frac{1}{\sqrt{2\pi\sigma^2}} \int_{-\infty}^{0} \exp \frac{-(x-\mu)^2}{2\sigma^2}\, dx \\ &= \frac{1}{2}\mathrm{erfc}\Big(\frac{\mu}{\sqrt{2}\sigma}\Big) \\ &= \frac{1}{2}\mathrm{erfc}\left(\sqrt{\Big(\frac{2\sigma^2}{\mu^2}\Big)^{-1}}\right) \\ &= \frac{1}{2}\mathrm{erfc}\left(\sqrt{\Big(2\cdot(\alpha+\beta+\gamma)\Big)^{-1}}\right) \end{aligned} \tag{A.20}$$

$$\begin{aligned} \alpha &= \frac{\sum_{n\in\mathbb{Z}_{\neq 0}} \Big\{p_t(\tau) * p_r(\tau)\Big\}^2_{\tau=nT}}{\Big\{p_t(\tau) * p_t(\tau)\Big\}^2_{\tau=0}} \\ \beta(\delta_\omega) &= \frac{\Big\{(p_t(-\tau) * p_t(\tau))\cdot\cos(\delta_\omega\tau)\Big\} * p_r(-\tau) * p_r(\tau)\Big|_{\tau=0}}{2T\Big\{p_t(\tau) * p_t(\tau)\Big\}^2_{\tau=0}} \\ \gamma(N_0, P_x) &= \frac{N_0\Big\{p_r(-\tau) * p_r(\tau)\Big\}_{\tau=0}\cdot\Big\{p_t(-\tau) * p_t(\tau)\Big\}_{\tau=0}}{2TP_x\Big\{p_t(\tau) * p_t(\tau)\Big\}^2_{\tau=0}} \end{aligned} \tag{A.21}$$

Appendix B

Extended results

Protocol	1.1	2.1	2.2	3.1	3.2	4.1	4.2	4.3	4.4
[Arisha:2002]			✓		✓	✓	✓	✓	✓
[Liu:2014]	✓	✓	✓	✓		✓		✓	✓
[Zhang:1993]	✓	✓		✓	✓	✓	✓	✓	✓
1-hopMAC	✓		✓			✓	✓	✓	✓
AD-MAC			✓			✓	✓	✓	✓
ADV-MAC			✓			✓	✓	✓	✓
AI-LMAC			✓			✓	✓	✓	✓
Alert	✓	✓	✓	✓	✓	✓		✓	✓
A-MAC	✓		✓	✓		✓	✓	✓	✓
AS-MAC			✓			✓	✓	✓	✓
ATL S-MACA	✓	✓	✓	✓		✓	✓	✓	
bitMAC	✓	✓	✓	✓	✓	✓	✓		✓
BMA			✓			✓	✓	✓	✓
B-MAC	✓		✓	✓	✓	✓	✓	✓	✓
BP-MAC	✓	✓	✓	✓	✓	✓	✓	✓	✓
BPS-MAC	✓	✓	✓	✓	✓	✓	✓	✓	✓
CC-MAC		✓	✓			✓	✓	✓	✓
CERA	✓	✓	✓	✓	✓	✓	✓		✓
C-MAC	✓	✓	✓	✓	✓	✓	✓	✓	
CMAC		✓	✓			✓	✓	✓	✓
Cognitive polling	✓	✓		✓	✓		✓	✓	✓
Contention-FDMA hybrid	✓	✓	✓	✓		✓	✓	✓	✓
Crankshaft			✓		✓	✓	✓	✓	✓
CSMA/ARC	✓	✓	✓		✓	✓	✓	✓	
CSMA/CA	✓	✓	✓	✓		✓	✓	✓	✓
CSMA/p*	✓	✓	✓	✓	✓	✓	✓	✓	

Protocol	**1.1**	**2.1**	**2.2**	**3.1**	**3.2**	**4.1**	**4.2**	**4.3**	**4.4**
CSMA-MPS	✓		✓	✓	✓	✓	✓	✓	✓
CSMA-TDMA Hybrid	✓	✓	✓	✓		✓	✓	✓	✓
DMAC		✓	✓		✓	✓	✓	✓	✓
DPCF-M		✓	✓			✓	✓	✓	✓
DPS-MAC			✓			✓	✓	✓	✓
DQRUMA	✓	✓	✓	✓		✓	✓	✓	✓
DSA++		✓	✓	✓		✓	✓	✓	✓
DSMAC			✓			✓	✓	✓	✓
DTMP		✓		✓	✓		✓	✓	✓
DW-MAC			✓			✓	✓	✓	✓
E2-MAC			✓			✓	✓	✓	✓
E2RMAC		✓		✓	✓	✓	✓	✓	✓
EMACs			✓		✓	✓	✓	✓	✓
EM-MAC			✓	✓	✓	✓	✓	✓	✓
ER-MAC		✓	✓		✓	✓	✓	✓	✓
ET-MAC	✓		✓	✓		✓	✓	✓	✓
EY-NPMA	✓	✓	✓	✓	✓	✓	✓	✓	✓
FASA	✓	✓	✓	✓	✓	✓	✓	✓	
FDMA	✓	✓	✓	✓	✓		✓	✓	✓
FLAMA			✓		✓	✓		✓	✓
FlexiMAC		✓	✓			✓	✓	✓	✓
f-MAC	✓	✓	✓	✓		✓	✓	✓	✓
FS-TS-Aloha	✓	✓	✓	✓	✓	✓	✓	✓	✓
FS-TU-Aloha	✓	✓	✓	✓	✓	✓	✓	✓	✓
FTDMA	✓	✓	✓	✓	✓		✓	✓	✓
Funneling-MAC		✓	✓			✓		✓	✓
FU-TS-Aloha	✓	✓	✓	✓	✓	✓	✓	✓	✓
FU-TU-Aloha	✓	✓	✓	✓	✓	✓	✓	✓	✓
G-MAC			✓		✓	✓	✓	✓	✓
HMAC			✓			✓	✓	✓	✓
HyMAC		✓	✓			✓	✓	✓	✓
IAMAC		✓				✓	✓	✓	✓
ISMA	✓	✓	✓	✓	✓	✓	✓	✓	✓
LEACH		✓	✓			✓	✓	✓	✓
LEEMAC		✓	✓		✓	✓	✓	✓	✓
LE-MAC			✓			✓	✓	✓	✓
LEMR			✓	✓	✓	✓	✓	✓	✓

Protocol	**1.1**	**2.1**	**2.2**	**3.1**	**3.2**	**4.1**	**4.2**	**4.3**	**4.4**
LLM			✓			✓	✓	✓	✓
LMAC			✓			✓	✓	✓	✓
LWT-MAC	✓		✓	✓	✓	✓	✓	✓	✓
MASCARA		✓	✓	✓		✓	✓	✓	✓
MC-LMAC			✓			✓	✓	✓	✓
MFP			✓	✓	✓	✓	✓	✓	✓
MH-MAC			✓	✓		✓	✓	✓	✓
MMAC			✓		✓	✓		✓	
MMSN		✓	✓		✓	✓	✓	✓	✓
MRPM				✓	✓	✓	✓	✓	✓
MSMAC			✓			✓	✓	✓	✓
MuChMAC			✓	✓		✓	✓	✓	✓
MX-MAC	✓		✓	✓	✓	✓	✓	✓	✓
nanoMAC	✓	✓	✓	✓		✓	✓	✓	✓
non persistent CSMA	✓	✓	✓	✓	✓	✓	✓	✓	✓
Optimized-MAC			✓			✓	✓	✓	
PACT		✓	✓			✓	✓	✓	✓
PAMAS	✓	✓	✓	✓		✓	✓	✓	✓
PCM	✓	✓	✓	✓		✓	✓	✓	✓
PEDAMACS			✓		✓	✓	✓	✓	✓
PMAC			✓			✓	✓	✓	
PRIMA		✓	✓			✓	✓	✓	✓
PRMA	✓	✓	✓	✓	✓		✓	✓	✓
PTIP		✓	✓	✓	✓	✓	✓	✓	✓
Pure Aloha	✓	✓	✓	✓	✓	✓	✓	✓	✓
PW-MAC		✓	✓	✓	✓	✓	✓	✓	✓
p-persistent CSMA	✓	✓	✓	✓	✓	✓	✓	✓	✓
QoS-MAC		✓	✓		✓		✓	✓	✓
RAMA	✓	✓	✓	✓		✓	✓	✓	✓
RAP	✓	✓	✓	✓	✓	✓	✓		✓
RATE EST			✓	✓		✓	✓	✓	
RC-MAC	✓		✓	✓		✓	✓	✓	✓
Reservation FS-ALOHA	✓	✓	✓	✓	✓		✓	✓	✓
RICER			✓	✓		✓	✓	✓	✓
RI-MAC	✓		✓	✓		✓	✓	✓	✓
R-ISMA	✓	✓	✓	✓		✓	✓	✓	✓
RIX-MAC	✓		✓	✓		✓	✓	✓	✓

Protocol	**1.1**	**2.1**	**2.2**	**3.1**	**3.2**	**4.1**	**4.2**	**4.3**	**4.4**
RL-MAC			✓			✓	✓	✓	✓
RMAC	✓	✓	✓	✓		✓	✓	✓	✓
RPMA	✓	✓	✓	✓	✓	✓	✓		✓
RRA-ISA	✓	✓		✓	✓		✓	✓	✓
RS-MAC	✓	✓	✓	✓		✓	✓	✓	✓
SCP-MAC			✓	✓	✓	✓	✓	✓	✓
SEESAW			✓			✓	✓	✓	✓
SIFT	✓	✓	✓	✓	✓	✓	✓	✓	✓
Slotted Aloha	✓	✓	✓	✓	✓	✓	✓	✓	✓
S-MAC			✓			✓	✓	✓	✓
S-MAC adaptive listening			✓			✓	✓	✓	✓
SOTP			✓			✓	✓	✓	✓
SPARE-MAC			✓			✓	✓	✓	✓
SpeckMAC-D	✓		✓	✓	✓	✓	✓	✓	✓
STEM-B	✓	✓		✓	✓	✓	✓	✓	✓
STEM-T	✓	✓		✓	✓	✓	✓	✓	✓
SyncWUF		✓	✓	✓	✓	✓	✓	✓	✓
TA-MAC			✓			✓	✓	✓	
TDMA	✓	✓	✓	✓	✓		✓	✓	✓
TICER			✓	✓		✓	✓	✓	✓
T-MAC			✓			✓	✓	✓	✓
TRAMA			✓		✓	✓		✓	✓
TrawMAC			✓	✓		✓	✓	✓	✓
TRIX-MAC	✓		✓	✓		✓	✓	✓	✓
U-MAC			✓			✓	✓	✓	
WiseMAC		✓	✓	✓	✓	✓	✓	✓	✓
X-MAC	✓		✓	✓	✓	✓	✓	✓	✓
Y-MAC			✓		✓	✓	✓	✓	✓
ZMAC		✓	✓			✓	✓	✓	✓
μ-MAC			✓	✓		✓	✓	✓	✓

Table B.1: Overview of MAC protocols.